

# 000 AUGMENTATIONS IN OFFLINE REINFORCEMENT 001 LEARNING FOR ACTIVE POSITIONING 002

003 **Anonymous authors**  
004

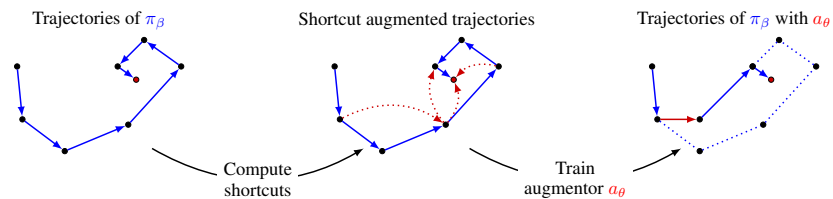
005 Paper under double-blind review  
006

## 007 ABSTRACT 008

009 We propose a method for data augmentation in offline reinforcement learning applied to active positioning problems. The approach enables the training of off-  
010 policy models from a limited number of trajectories generated by a suboptimal  
011 logging policy. Our method is a trajectory-based augmentation technique that ex-  
012 ploits task structure and quantifies the effect of admissible perturbations on the  
013 data using the geometric interplay of properties of the reward, the value function,  
014 and the logging policy. Moreover, we show that by training an off-policy model  
015 with our augmentation while collecting data, the suboptimal logging policy can  
016 be supported during collection, leading to higher data quality and improved off-  
017 line reinforcement learning performance. We provide theoretical justification for  
018 these strategies and validate them empirically across positioning tasks of varying  
019 dimensionality and under partial observability.  
020

## 021 1 INTRODUCTION 022

023 In active positioning, an end-effector must place an object precisely at a desired pose. Such prob-  
024 lems occur in high-precision manufacturing, e.g., in camera Bräuniger et al. (2014) or telescope  
025 assembly Upton et al. (2006), in alignments of laser optics Rakhmatulin et al. (2024), as well as in  
026 many robotic manipulation tasks Plappert et al. (2018). In optical systems, this involves iterative  
027 adjustment of components, such as lenses or mirrors, to maximize alignment quality from image-  
028 based signals. These tasks are naturally modeled as contextual partially observed Markov decision  
029 problems (POMDPs) and demand generalization over the context Burkhardt et al. (2025). While  
030 reinforcement learning (RL) has advanced algorithmically, online training is costly: explorations in  
031 high-dimensional observation and continuous action spaces are inefficient, cause long downtimes,  
032 and human interaction is often required between episodes, for instance to insert new objects. At the  
033 same time, precise but inefficient expert routines can provide data, making offline RL a promising  
034 alternative, which sidesteps online interactions by training from pre-collected datasets(Levine et al.,  
035 2020). Although offline RL promises to learn policies better than the logging policy from static  
036 datasets, without online interactions, it suffers from distributional shifts and inappropriate datasets,  
037 leading to suboptimal policies. To cope with distribution shift, contemporary offline RL methods  
038 regularize policies toward the behavior distribution or warm-start from the logging policy before  
039 cautiously improving it (see Section 1.2 for an overview).  
040



043 Figure 1: Overview of LIFT.  
044

045 Despite these algorithmic advances, it remains unclear how the data-generating logging policy limits  
046 what an offline learner can achieve. Prior evidence already shows that dataset selection can dominate  
047 algorithmic differences (Schweighofer et al., 2022; Fu et al., 2021; Yarats et al., 2022); actionable  
048

guidance for improving the data itself, however, remains scarce. Moreover, when probing effects of logging policies, prior work typically uses different categories of expertness where often the data of highest expertness is produced by an RL agent trained online (Fu et al., 2021). Although this schema is convenient, it could introduce a methodology bias: the generated trajectory inherits the exploration style and failure modes of the training algorithm, not those of deterministic, production-grade expert routines common in practice. Mixing datasets of different quality not only degenerates performance, it can also practically be infeasible to hand-off between policies. For instance, expert systems typically are deterministic, tightly scripted routines with internal states where decisions can depend on the entire trajectory of measurements. Inserting actions in-between can invalidate the routine’s assumptions and it only be able to resume reliably if it restarts from the new state.

In this work, we design data-efficient RL methods for active positioning tasks that can effectively learn from *inefficient* expert policies that can precisely place objects but need many steps to do so. Our key idea is to augment the logging policy sparingly with actions proposed by an off-policy learner trained parallel to the data collection. The off-policy learner is trained in a way to explore shortcuts in the experts trajectories to make hand-offs seamless and effective.

### 1.1 CONTRIBUTIONS

We introduce *LIFT*, short for logging improvement via fine-tuned trajectories, a framework that enhances punctual data collection for offline RL. Specifically, we propose a novel augmentation scheme (Section 4) that keeps the logging policy in control while enabling optimistic probing by an augmentor trained as data is collected. The augmentor’s goal is to skip redundant and unnecessary sub-trajectories during collection and to smooth hand-offs between itself and the logging policy. A key challenge is to train the augmentor with very limited data so that such *shortcuts* can be identified punctually. Our idea is to train the augmentor on synthetic trajectories obtained from real data that exhibit such shortcuts. We prove in Section 3 under which conditions such shortcuts can be reliably identified in logged data, and we devise an algorithm to extract them from this data (Algorithm 1). Finally, Section 5 presents a systematic study that underlines the strength and generality of our approach by analyzing the effect of the logging policy, transition behavior, dimensionality, and informativeness of observations on policy performance across a diverse class of active positioning tasks. We implemented the shortcut augmentation in d3rlpy Seno & Imai (2022), following its transition picker protocol, which allows our static augmentation method to be integrated into any RL algorithm implemented in d3rlpy by adding a single line of code.<sup>1</sup>

### 1.2 RELATED WORK

A central challenge in offline RL is overestimating values for out-of-distribution actions. Methods address this either by constraining the learned policy toward the logging distribution or by learning pessimistic value functions. Representative approaches include behavior regularization via BC losses or divergence penalties (Fujimoto et al., 2019; Fujimoto & Gu, 2021; Tarasov et al., 2023), pessimistic critics (Kumar et al., 2020), or expectile-based policy extraction (Kostrikov et al., 2022). Methods depending on regularizations are sensitive to hyperparameters and they often limit the policy to stay close to the behavior, for instance due to safety constraints, which can be detrimental if the behavior is highly suboptimal. Moreover, several studies note that algorithm performance is highly sensitive to dataset composition (Fu et al., 2021; Hong et al., 2023), that is, mixing suboptimal trajectories with expert data. Prior work has studied intensively the importance of high-coverage Yarats et al. (2022); Wagenmaker et al. (2025) and expertness of datasets Kumar et al. (2022); Corrado et al. (2024) for offline RL. This has been underpinned by the investigations in Schweighofer et al. (2022), where scores are designed that measure exploitation and exploration capabilities of datasets and how these affect algorithmic performance of offline RL methods. Increasing the dataset diversity via data augmentations is another line of work to mitigate narrow data distributions. In Andrychowicz et al. (2017), an augmentation scheme for sparse reward in robotic manipulation tasks is proposed that re-labels goals and states in logged trajectories to create additional successful transitions. Augmentations for problems with image observations have been studied extensively in the literature, were it was shown that rather simple image augmentations Laskin et al. (2020); Sinha et al. (2022), like

<sup>1</sup>The implementations are included in the supplemental material of this submission and will be made available on GitHub upon acceptance.

random or utilizing causal techniques Pitis et al. (2020) can significantly improve sample efficiency. Recently, diffusion-based techniques have been proposed that generate synthetic trajectories in order to make offline RL more robust Li et al. (2024); Lee et al. (2024); Lu et al. (2023). Different than purely *offline* augmentations generating synthetic data from static datasets and more relevant for our work are hybrid schemes actively enhance the data collection process itself. The easiest hybrid scheme is to warm-start online RL from an offline-trained policy, then continue by adding newly collected online. Prior work shows that this, in combination with a careful sampling scheme and network architecture Ball et al. (2023) or policy regularizations Nair et al. (2018), can turn offline data into a strong initializer for online learning. Nevertheless, these methods still require rather long online fine-tuning or high-quality offline datasets, neither of which is typically available in active positioning tasks. A more subtle scheme is to let an expert guide the data collection process, like in GuDA Corrado et al. (2024), where human-guidance is interleaved to direct trajectories toward success. Another relevant line of work is to weave online transitions into logging policies as in iterative offline RL (IORL) (Zhang et al., 2023). Here, exploratory actions are injected to discover unexplored regions in state-action space while training an offline RL agent on the generated trajectories. This approach is discussed in Section 4. Our approach is similar in spirit, but instead of exploring we want to exploit shortcuts in the trajectories to make hand-offs seamless and effective.

## 2 ACTIVE POSITIONING

In this section, we introduce the specific framework for active positioning problems building upon the framework for active alignments introduced in Burkhardt et al. (2025). There, active positioning problems are modelled as an *episodic* and *contextual* POMDP Modi et al. (2018). Specifically, the state is decomposed in the current position  $s \in \mathcal{P}$  with  $\mathcal{P}$  a bounded subset of  $\mathbb{R}^m$  and a static context parameter  $W \in \mathcal{W}$ , that is  $\mathcal{S} = \mathcal{P} \times \mathcal{W}$ . The actions can be selected from a subset  $\mathcal{A}$  of  $\mathbb{R}^d$ . Applying an action  $a \in \mathcal{A}$  at state  $(s, W)$  gives the new state  $(s', W)$  with  $s' = f(s, a, W)$ , where  $f : \mathcal{P} \times \mathcal{A} \times \mathcal{W} \rightarrow \mathbb{R}^d$  a parametrized *distortion function*. Typically, any position can be reached from any other position within one action. Note that in our scenarios, the action space is additive, meaning that the sum of two actions is itself an action if its in  $\mathcal{A}$ . Throughout we assume that  $f(s, 0, W) = s$ . Our running example is  $f(s, a, W) = s + W \cdot a$  with  $W \in \mathbb{R}^{d \times d}$  a distortion matrix, like a rotation matrix, but we will also consider non-linear distortions. Importantly, as  $W$  stay constant throughout each episode, so is the extent of the distortion. One can think of  $W$  as variances introduced by the gripping of an object, variances within an object, or conditions of the goal to be reached. In each episode, the goal is to navigate from a random initial position  $s_0$  and randomized context  $W$  to a terminal state  $s_W \in \mathbb{R}^d$ . The reward observed at state  $(s, W)$  is  $R(s, a, W) = -\|f(s, a, w) - s_W\|$ , i.e. the negative distance to the terminal state. An episode ends once the state is sufficiently close to  $s_W$  or an upper limit of steps is reached. Formally, we terminal states are all within the set  $\{(s, W) \in \mathcal{S} : \|s - s_W\| \leq \theta\}$ . Typically,  $W$  cannot be observed directly, often even  $s$  cannot. Instead, an often high-dimensional and noised output  $O_W(s) \in \mathcal{O}$  is observed, which is controlled by a conditional probability density function depending on  $s$  and  $W$ . In total, we call the tuple  $(\mathcal{P}, \mathcal{W}, \mathcal{O}, f, \gamma)$  an *active positioning problem*. This framework covers various industrial use cases, from robot arm positioning, to active alignments of optical devices (Figure 2).

Although active positioning problems can also be considered as black-box optimization problems Burkhardt et al. (2025), they are inherently RL problems where symmetries and ambiguities in the need to be actively explored. For instance, the observation space is typically highly symmetric and context-dependent: states  $s$  and  $s'$  that are far apart can yield very similar observations  $O(s, W) \approx O(s', W)$ , while the same state can produce very different observations  $O(s, W)$  and  $O(s, W')$  under different contexts. Additionally, safety constraints and physical limitations often restrict the action space  $\mathcal{A}$  so that the optimal state cannot be reached in one step and a sequence of informed actions is required. In the RL formulation, a *policy*  $\pi : \mathcal{A} \times \mathcal{O} \rightarrow \mathbb{R}$  is a mapping of observations and actions to likelihood and the dynamics of the combined sys-

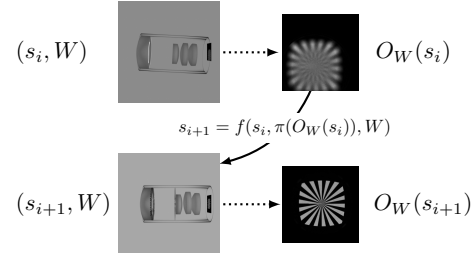


Figure 2: Active positioning of a lens system, taken from Burkhardt et al. (2025)

162 tem works as follows: At a given state  $(s, W)$ ,  $O(s, W)$  is observed and an action  $a$  is sam-  
 163 pled from  $\pi(\cdot, O(s, W))$ . The system then moves to the new state  $s' = f(s, a, W)$ . Note that  
 164  $a$  and  $s$  do not need to have same dimensionality. Starting from state  $(s_0, W) \in \mathcal{S}$ , the com-  
 165 bined dynamics yields a trajectory  $(s_0, W), \dots, (s_k, W)$ . The goal is to find a policy  $\pi$  maxi-  
 166 mizing  $J(\pi) := \mathbb{E}_{s_0, W} \left[ \sum_{i=0}^k -\gamma^i \|s_i - s_W\| \right]$ , where  $\gamma \in (0, 1)$  is a *discount factor*. Clearly,  
 167  $J(\pi) = \mathbb{E}_{s_0, W} [V^\pi(s_0, W)] = \mathbb{E}_{s_0} [V^\pi(s_0)]$  with  $V^\pi$  the state-value function and  $V^\pi(s) :=$   
 168  $\mathbb{E}_{W \sim \mathcal{W}} [V^\pi(s, W)]$ . Similarly, we define the state-action value functions  $Q^\pi(s, a, W)$  and  $Q^\pi(s, a)$ .  
 169

### 170 171 3 THEORETICAL ANALYSIS OF SHORTCUT AUGMENTATIONS

172 In active positioning, good trajectories reach the optimal position in as few steps as possible. Al-  
 173 though most logging policies used in applications visit states that are close to the optimal state,  
 174 they often produce long and redundant trajectories. Our core idea is to train agents on synthetic  
 175 trajectories distilled from these imperfect data, which are more direct and goal-reaching. Intuitively,  
 176 we want the agent to *skip* parts of the trajectory that do not add much value — for example, going  
 177 straight instead of replicating zig-zag movements or detours present in the logged data (Figure 1).  
 178 However, improving logged trajectories is not straightforward. For instance, assume a collected tra-  
 179 jectory of a logging policy contains a sub-trajectory  $(s_i, W), (s_{i+1}, W), \dots, (s_j, W)$  with actions  
 180  $a_i, \dots, a_{j-1}$ , representing a long detour, like a zig-zag movement, from  $s_i$  to  $s_j$ . Clearly, going  
 181 directly from  $s_i$  to  $s_j$  would yield a trajectory with higher return. However, naively applying the  
 182 accumulated action  $a = a_i + a_{i+1} + \dots + a_{j-1}$  at  $s_i$  will not necessarily land exactly at  $s_j$  due  
 183 to distortions in the dynamics induced by  $f$ . Even small misplacements, that is ending up close to  
 184  $s_j$  but not exactly at  $s_j$ , can cause significant value degradation if the value function is not stable in  
 185 the vicinity of  $s_j$ . Worse, applying  $'$  at  $s_i$  may even move us in the opposite direction, away from  
 186  $s_j$ , with no guarantee that the new state has a higher value than  $s_i$ . Here, the length of the action  
 187  $'$ , the value gap between  $s_i$  and  $s_j$ , the stability of the value function around  $s_j$ , and the distortion  
 188 in the dynamics at  $s_i$  all play a role. This section is about when the accumulated action  $a$  is indeed  
 189 beneficial. To start, we first formalize what it means for an action to be beneficial in our setting. We  
 190 call a policy  $\pi$  *distance-improving*, if for all  $W \in \mathcal{W}$  we have for two subsequent states  $(s_i, W)$  and  
 191  $(s_j, W)$ , with  $i < j$  visited by the policy that  $\|s_j - s_W\| < \|s_i - s_W\|$ . In other words, the reward  
 192 along a trajectory of  $\pi$  is strictly increasing. In this section, we restrict to deterministic policies  
 193 which most logging policies are. Given the deterministic transition dynamics given by  $f$ , the value  
 194 function  $V^\pi(s, W)$  is exactly the return of  $\pi$  starting from  $(s, W)$ .

195 **Proposition 3.1.** *Let  $\pi$  be a distance-improving policy and  $(s, W), (s', W) \in \mathcal{S}$  two states on a  
 196 trajectory of  $\pi$  where  $(s, W)$  is visited prior to  $(s', W)$ , then  $\gamma V^\pi(s', W) - V^\pi(s, W) \geq \|s' - s_W\|$ .*

197 All proofs are in Section A. Restricting the focus on distance-improving logging policies, beneficial  
 198 actions for active positioning problems can be defined as follows:

199 **Definition 3.1.** *Let  $\pi$  be a policy,  $(s, W) \in \mathcal{S}$  a state, and  $a \in \mathcal{A}$  an action with  $s' = f(s, a, W)$ . If  
 200  $\gamma V^\pi(s', W) - V^\pi(s, W) \geq \|s' - s_W\|$ , then  $a$  is a  $\pi$ -shortcut at  $(s, W)$ .*

202 Note that shortcuts depend on the latent information  $W$ , not on the position alone. The remainder of  
 203 this section studies how to find shortcuts in offline trajectories. To do so, consider a short trajectory  
 204  $(s_0, W), (s_1, W), (s_2, W)$  from a distance-improving policy  $\pi$  with actions  $a_0$  and  $a_1$  (Figure 3a).  
 205 In principle, an action  $a$  with  $s_2 = f(s_0, a, W)$  is a shortcut (Definition 3.1) and thus beneficial.  
 206 However, due to distortion in  $f$ , we cannot assume  $a = a_0 + a_1$ , nor that applying  $a_0 + a_1$  at  $s_0$   
 207 will reach  $s_2$ . We must at least ensure that  $a_0 + a_1$  indeed leads near  $s_2$  which requires to control  
 208 placement errors induced by  $f$ . In case  $f(s, a, W) = s + W \cdot a$  with  $W \in \mathbb{R}^{m \times d}$ , trajectories can  
 209 be augmented without placement errors:

210 **Proposition 3.2.** *Let  $f(s, a, W) = s + W \cdot a$  and let  $(s_i, W)$  and  $(s_j, W)$  with  $i < j$  on a trajectory  
 211 of a distance improving policy  $\pi$  and  $a_i, \dots, a_{j-1}$  the chain of actions  $\pi$  undertook to get from  $s_i$  to  
 212  $s_j$ . Then  $a = \sum_{k=i}^{j-1} a_k$  is a shortcut for  $s_i$ .*

214 Extending Proposition 3.2 to non-linear dynamics is not trivial. Generally, we want to have that  
 215 accumulating actions along a trajectory does not lead to too much placement uncertainty, which is  
 typically the case in real-world positioning problems. We formalize this as follows:

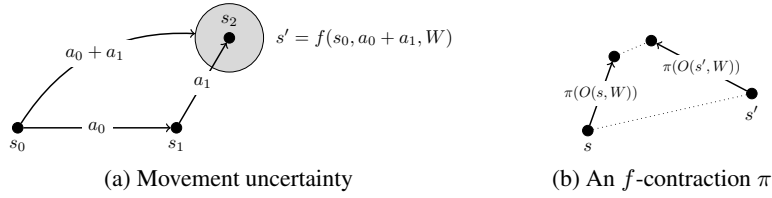


Figure 3: Interactions of policy with movement dynamics.

**Definition 3.2** (Linear placement-errors). A distortion function  $f$  has *linear placement-errors* (LPE) if there exists a constant  $L_f$  such that for any chain of actions  $a_0, \dots, a_{k-1}$  with  $\hat{a} := \sum_{i=0}^{k-1} a_i \in \mathcal{A}$  executed on  $(s_0, W)$  with  $s_i = f(s_{i-1}, a_{i-1}, W)$ , we have:  $\|f(s_0, \hat{a}, W) - s_k\| \leq L_f \cdot \sum_{i=0}^{k-1} \|a_i\|$ .

Intuitively, the LPE property means that although a system distort movements, the mismatch introduced when regrouping actions cannot grow faster than linearly with the size of the path taken. This actually includes a wide range of functions where the distortion depends on the state only:

**Proposition 3.3.** *Let  $f(s, a, W) = s + g(s, W) \cdot a$  with  $g : \mathcal{S} \rightarrow \mathbb{R}^{m \times d}$  a bounded matrix-function. Then  $f$  has LPE with  $L_f = 2 \cdot \sup_{\mathcal{S}} \|g\|$ .*

As we will see, when the distortion term also depends on the action, i.e.  $g(s, a, W)$ , things become more involved for small actions  $a$  even if  $g$  is bounded and LPE does not follow without additional assumptions (see Section 5.1.1). In Proposition B.1, we introduce an even stronger property which suffice to imply LPE for distortion functions of common active positioning problems, like linear movement dynamics. More specifically, it follows directly that a linear movement-dynamics of the form  $f(s, a, W) = s + Wa$  has LPE with  $L_f = 0$ .

Having gathered a notion of placement errors, we now need to control the stability of the value function. Specifically, even when we can precisely reach  $s_j$  from  $s_i$ , the value function  $V^\pi$  can change drastically in the vicinity of  $s_j$ , making it hard to guarantee that applying the accumulated action  $a$  at  $s_i$  is indeed beneficial. To control this, we have to impose good properties on  $V^\pi$ . We call a value function  $V : \mathcal{S} \rightarrow \mathbb{R}$   *$L_V$ -Lipschitz continuous* if for all  $(s, W), (s', W) \in \mathcal{S}$  we have  $|V(s, W) - V(s', W)| \leq L_V \cdot \|s - s'\|$ . This is the final ingredient to prove our main statement:

**Theorem 3.4.** *Let  $\pi$  be distance improving and assume that  $V^\pi$  is  $L_V$ -Lipschitz continuous and  $L_f$ -placement errors. Let  $(s_i, W)$  and  $(s_j, W)$  on a trajectory of  $\pi$  and let  $a = \sum_{k=i}^{j-1} a_k$  be the sum of the chain of actions  $\pi$  undertook to get from  $s_i$  to  $s_j$ . Then  $a$  is a  $\pi$ -shortcut for  $s_i$  if*

$$\gamma \cdot V^\pi(s_j, W) - V^\pi(s_i, W) - \|s_j - s_W\| \geq (\gamma \cdot L_V + 1) \cdot L_f \cdot \sum_{k=i}^{j-1} \|a_k\|.$$

In some sense, Proposition 3.2 for movement dynamics of the form  $f(s, a, W) = s + W \cdot a$  arises as a special case of Theorem 3.4 because  $L_f = 0$  implies that the right-hand side becomes 0 and the left-hand side is always non-negative due to Proposition 3.1. However, we note that Theorem 3.4 requires  $V^\pi$  to be Lipschitz continuous, which is not needed in Proposition 3.2.

So far, we have not made any direct assumptions on policy  $\pi$  beside being distance improving and  $V^\pi$  being Lipschitz continuous. The next condition helps to ensure that  $V^\pi$  is indeed Lipschitz continuous (see Proposition A.2 in Section A), which requires a beneficial interplay with  $f$ :

**Definition 3.3** ( $f$ -contraction). We call a policy  $\pi$  an  *$f$ -contraction* if for all pairs  $(s, W), (s', W)$  with respective observations with  $o = O(s, W)$  and  $o' = O(s', W)$ , we have

$$\|f(s, \pi(o), W) - f(s', \pi(o'), W)\| \leq \|s - s'\|.$$

**Corollary 3.5.** *Let  $\pi$  be distance improving  $f$ -contraction and let  $f$  have LPE with constant  $L_f$ . Let  $(s_i, W)$  and  $(s_j, W)$  on a trajectory of  $\pi$  and let  $a = \sum_{k=i}^{j-1} a_k$  be the sum of the chain of actions  $\pi$  undertook to get from  $s_i$  to  $s_j$ . Then  $a$  is a shortcut for  $s_i$  if*

$$\gamma \cdot V^\pi(s_j, W) - V^\pi(s_i, W) - \|s_j - s_W\| \geq \frac{L_f}{1 - \gamma} \cdot \sum_{k=i}^{j-1} \|a_k\|$$

270 Being an  $f$ -contraction is a stronger requirement than mere distance improvement. We refer to  
 271 Section B.2 for a discussion and examples of  $f$ -contractions and Lipschitz value functions in real-  
 272 world policies. In practice, many active positioning policies do not satisfy the contraction property  
 273 globally, yet this is not required for identifying useful shortcuts as shown in our experiments.  
 274

## 275 4 LOGGING IMPROVEMENTS VIA FINE-TUNED TRAJECTORIES

277 The idea of iterative reinforcement learning is to enrich logging policies with exploratory steps while  
 278 collecting data (Zhang et al., 2023), mostly in order to improve coverage of the state-action space.  
 279 Specifically, an *uncertainty model*  $E_\theta(s, a)$  is trained with  $E_\theta(s, \cdot)$  a probability distribution on  $\mathcal{A}$  for  
 280 each  $s \in S$ . Given a dataset  $D$ ,  $E_\theta$  is trained by minimizing  $\mathbb{E}_{(o, a) \sim D} [-\log(E_\theta(s, a)) + \mathcal{R}(\theta)]$  with  
 281  $\mathcal{R}(\theta)$  a regularization term. Intuitively,  $E_\theta(s, a)$  can be seen as the probability that action  $a$  has been  
 282 seen for state  $s$  in  $D$ . Actions with small probability  $E_\theta(s, a)$  at state  $s$  are considered as exploratory  
 283 action and should be selected according to some fixed probability  $p$  enriching a given logging policy  
 284  $\pi_\beta$  during rollout. These *exploratory actions* are rather rare and thus help keeping the system save  
 285 and naturally close to the logging policy  $\pi_\beta$  that generated the data. Although this approach seems  
 286 appealing, a central part that has been underexplored in current literature, namely that static logging  
 287 policies may not deal well with intermediate exploratory steps. In practise, arbitrary exploratory  
 288 steps may lead to states where the logging policy cannot recover well from, leading to lower overall  
 289 returns. We build upon this idea, but instead of selecting actions that have not been seen in the  
 290 data, we advocate to train a  $Q$ -function  $Q_\theta$  on some initial dataset  $D$  and select actions having high  
 291  $Q$ -values. Formally, we set  $a_\theta(s, a) = \max_{a' \in \mathcal{A}} Q_\theta(s, a')$  where  $Q_\theta$  can be trained with any offline  
 292 RL method, like CQL or IQL. We call  $a_\theta$  an *augmentor*. By that, we aim to enrich the dataset with  
 293 actions that are likely to be beneficial for  $\pi_\beta$  in the sense of higher returns. While this idea is quite  
 294 universal and it remains unclear how action that ease hand-overs look like in general. Moreover, in  
 295 order that the augmentor provides useful steps, it has to be trained well already with limited data.  
 296 The idea of LIFT to show the augmentor data of *good behavior* by applying augmentation to the  
 297 logged data that emphasizes such behavior. Its easy to show that when  $a_\theta$  to suggest  $\pi_\beta$ -shortcuts  
 298 (Definition 3.1), a better logging policy can be obtained:

299 **Proposition 4.1.** *Let  $\pi_\beta$  and  $a_\theta$  be two policies, then  $J(\pi_{\text{aug}}) \geq J(\pi_\beta)$  with  $\pi_{\text{aug}}$  defined as follows:*

$$300 \pi_{\text{aug}}(O(s, W)) := \begin{cases} a_\theta(O(s, W)) & \text{if } a_\theta(O(s, W)) \text{ is a } \pi_\beta\text{-shortcut at } (s, W) \\ 301 \pi_\beta(O(s, W)) & \text{otherwise} \end{cases}.$$

303 This can be seen a special case of the policy improvement theorem (Sutton & Barto, 2018, Sec-  
 304 tion 4.2) to active positioning. For the remainder of this section, we discuss how to train  $a_\theta$  in order  
 305 that it suggests  $\pi_\beta$ -shortcuts for active positioning problems. However, we want to emphasize that  
 306 LIFT in general is not tied to this form of backbone-augmentations.

307 Theorem 3.4 gives a condition when and how to augment a trajectory  $(o_0, a_0, r_0), \dots, (o_n, a_n, r_n)$   
 308 with latent states  $s_i = f(s_{i-1}, a_{i-1}, W)$ , observations  $o_i = \mathcal{O}(s_i, W)$ , rewards  $r_i = -\|s_{i+1} - s_W\|$ ,  
 309 and actions  $a_i = \pi_\beta(o_i)$  from a logging policy  $\pi_\beta$ . To convey them into a practical algorithm, let  
 310  $C \in \mathbb{R}_{\geq 0}$  be a constant and let  $G_i = V^\pi(s_i, W) = \sum_{k=i}^n \gamma^{k-i} r_k$  be the returns of  $\pi_\beta$ . Now, take  
 311 any pair  $(i, j)$  with  $i < j$ , let  $\hat{a} = \sum_{k=i}^{j-1} a_k$  be a shortcut candidate and check if  $\gamma G_j - G_i + r_{j-1} \geq$   
 312  $C \cdot \sum_{k=i}^{j-1} \|a_k\|$  with some constant  $C$  holds true. Clearly, without prior information on  $f$  and  $\pi_\beta$ , the  
 313 exact value of  $C$  remains unclear, and thus it has to be considered a regularization hyperparameter  
 314 of our method. If  $C = 0$ , all pairs are considered shortcuts, if  $C$  is large, only very few pairs where  
 315 high reward is gained in a few short steps are considered shortcuts. If the inequality is valid for  $(i, j)$ ,  
 316 we can assume that  $\hat{a}$  is a shortcut and ideally, we would add the tuple  $(o_i, \hat{a}, -\|s'_j - s_W\|, o'_j)$  with  
 317  $s'_j = f(s_i, \hat{a}, W)$  and  $o'_j = \mathcal{O}(s'_j, W)$  to the dataset. However, due to the movement uncertainty,  
 318 there is a gap between the position  $s'_j$  the shortcut leads to and the observed state  $s_j$ . Particularly,  
 319 the image observation  $\mathcal{O}(s'_j, W)$  and the reward  $-\|s'_j - s_W\|$  differ from the actually observed ones,  
 320 namely  $o_j$  and  $r_{j-1}$ . We argue, however, that in many practical applications, this gap is small, for  
 321 instance if  $L_f = 0$  as in linear movement dynamics  $f(s, a, W) = s + W \cdot a$  (see Proposition 3.2).  
 322 Thus, we add  $(o_i, a, r_{j-1}, o_j)$  to the training dataset. Algorithm 1 summarizes our shortcut sampling  
 323 procedure, and we want to emphasize that it can be added to any offline RL method that samples  
 from an offline dataset, like to minimize the Bellman error or related temporal difference errors as

324 in CQL. Note that for a given input tuple, the runtime of Algorithm 1 is  $O(n)$ . Observe that the  
 325 synthetic shortcuts are only used to obtain the augmentor  $a_\theta$ , which in turn is only used to fine-tune  
 326 the logging policy, and the collected dataset consists of real data only. The precise procedure is  
 327 described in Algorithm 2. For that, they must have good hand-over properties and thus we augment  
 328 the dataset  $D$  with shortcuts computed via Algorithm 1 when training  $Q_\theta$ .  
 329

---

**Algorithm 1:** Shortcut sampling
 

---

330 **Input** :  $C \geq 0, i \in [n]$ , trajectory  
 331  $\{(o_0, a_0, r_0), \dots, (o_n, a_n, r_n)\}$   
 332  
 333 **Output** : Tuple  $(o_i, \hat{a}, r_{j-1}, o_j)$   
 334 Compute returns  $G_0, \dots, G_n$  for  
 335 trajectory  
 336  $S = \{\}$   
 337 **for**  $j = i + 1 \dots n$  **do**  
 338    $\hat{a} \leftarrow \sum_{k=i}^{j-1} a_k$   
 339   **if**  $\gamma G_j - G_i \geq C \cdot \sum_{k=i}^{j-1} \|a_k\|$  and  
 340     $\hat{a} \in \mathcal{A}$  **then**  
 341     | Add  $(o_i, \hat{a}, r_{j-1}, o_j)$  to  $S$   
 342 Let  $m = |S|$  and denote  $\hat{r} = (\hat{r}_1, \dots, \hat{r}_m)$   
 343 the rewards of the tuples in  $S$   
 344 Let  $p \sim \hat{r} - \min \hat{r}$  a mass function  
 345 Sample  $(o_i, \hat{a}, r_{j-1}, o_j)$  from  $S$  w.r.t.  $p$   
 346 **return**  $(o_i, \hat{a}, r_{j-1}, o_j)$ 


---

 351 **5 EXPERIMENTS**

352  
 353 To evaluate LIFT for active positioning problems, we address two main questions: First, can short-  
 354 cut augmentations improve pure offline RL, and second, can they be leveraged during data collection  
 355 by training a  $Q$ -based augmentor in comparison to warm-start RL? To this end, we test different dis-  
 356 tortion functions  $f$ , observation types  $\mathcal{O}$ , and levels of expertness of the logging policies.  
 357

 358 **5.1 ENVIRONMENTS**

359 In order to analyze different movement distortions and observation types in isolation, we conducted  
 360 our experiments in semi-realistic active positioning environments designed to keep real world char-  
 361 acteristics and entail small sim-to-real gaps. Throughout, we use  $-\|s - s_W\|$  as reward signal, which  
 362 is easy to compute in simulations, as one typically has access to latent information  $(s, W)$ .  
 363

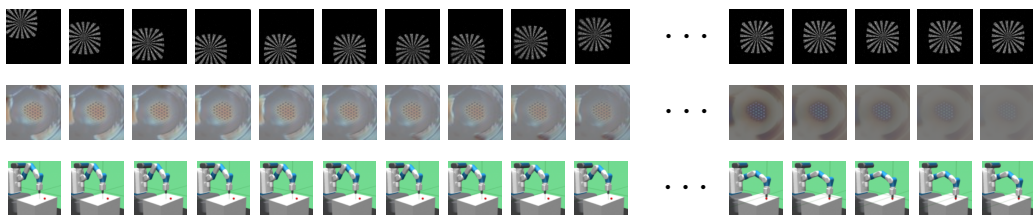
 364 **5.1.1 MOVEMENT DISTORTIONS**

365 We consider different movement distortions, some of them have linear forms, like  $f_{\text{blend}}$  and  $f_{\text{rot}}$  both  
 366 with  $L_f = 0$ . We also use non-linear distortions, like  $f_{\text{scale}}$  and  $f_{\text{sin}}$  which have LPE with  $L_f > 0$   
 367 and one non-continuous distortion  $f_{\text{regrot}}$  also having LPE which is not contracting. We also test  
 368 a movement dynamics, called  $f_{\text{sqrt}}$ , that does not satisfy the LPE property. We refer to Section B  
 369 for their precise mathematical definitions and corresponding proofs of their properties. Figure 6  
 370 illustrates an overview of the different distortions in two dimensions.  
 371

 372 **5.1.2 OBSERVATIONS**

373 A canonical type of observation is when the position can be observed directly, i.e.,  $\mathcal{O}_{\text{PO}}(s, W) = s$ .  
 374 Here, we have to fix optimum  $s_W = s^*$  throughout, as otherwise it is impossible to infer where the  
 375 optimum should be without observing information about  $W$ . Roughly speaking, these are scenarios  
 376 where it is known where the optimum is, but not how to get there. We will evaluate these scenarios  
 377 in  $d = 2$  and  $d = 5$  dimensions. Our motivation stems from scenarios where observations are drawn

378 from optical sensors and hence we test our method on different image generators (Figure 4). The  
 379 first comes from active alignments problems from camera assembly, were a lens objective has to  
 380 be positioned relative to a sensor to obtain optimal optical performance Liu et al. (2024). Here,  $s$   
 381 relates to the position of the lens objective and  $W$  to variances in the lenses of the objective and  
 382 distortions in the movement dynamics. At each position  $s$ , light is sent through the lens system  
 383 creating an image  $\mathcal{O}_{LP}(s, W)$  on a sensor. The task is to position the objective with variances  $W$   
 384 precisely to an individual optimum  $s_W$  (Figure 2) As some information about  $W$  is contained in  
 385 the image implicitly, it is possible to design algorithms that leverage the image information to move  
 386 towards  $s_W$ . We use the realistic generator from Burkhardt et al. (2025) where collimated light is  
 387 sent in the form of a *Siemens star* producing images whose contrast and sharpness are sensitive to  
 388 small misalignments, thereby providing a rich and informative signal for learning-based control.  
 389



397 Figure 4: Exemplary trajectories of  $\pi_{cw,l}$  executed in  $\mathcal{O}_{LP}$ ,  $\mathcal{O}_{LT}$ , and  $\mathcal{O}_{RI}$  (top to bottom).  
 398

399 Our second image generator is the *light tunnel* from Gamella et al. (2025), where light is sent from  
 400 a source through two polarizers whose angles dictate how light passes through to an optical sensor.  
 401 Here, each position  $s$  of the polarizers filters out certain wavelengths of the light creating a  
 402 image  $\mathcal{I}(s)$  at the sensor. Here, the image observation does not depend on the context  $W$  and  
 403 essentially only on the relative difference of the angles of the polarizers, i.e. many states lead to the  
 404 same image. To add some context, we sample in each episode  $s_W$  uniformly from the box  $[0, 2\pi]^2$   
 405 and set  $\mathcal{O}_{LT}(s, W) = \mathcal{I}(s) - \mathcal{I}(s_W)$ . In our experiments, we use the decoder of the autoencoder  
 406 trained on images from the real system provided in the data repository of Gamella et al. (2025).  
 407

408 Lastly, we run experiments in the *Fetch Reach* environment Plappert et al. (2018), where a robotic  
 409 arm has to reach a position  $s_W$ . Here, we use the vanilla environment  $\mathcal{O}_{RP}(s, W) = s - s_W$  where  
 410 the distance to the target is observed. In Section C we study the effect of shortcut augmentation for  
 411 harder variants using image observations and reaching multiple goals subsequently.  
 412

### 5.1.3 LOGGING POLICIES

414 Algorithms for active positioning do not follow a general  
 415 recipe, but rather depend on the specific application. Alignments  
 416 of optical systems, for instance, have traditionally relied  
 417 on iterative optimization of measured performance  
 418 signals such as coupling efficiency or spot quality, where  
 419 actuators are moved sequentially or in small patterns and the  
 420 response is evaluated to guide subsequent steps, typically following  
 421 coordinate-descent or heuristic search strategies that  
 422 explore one or more degrees of freedom at a time (Parks,  
 423 2006; An et al., 2021; Langehanenberg et al., 2015).  
 424

425 Typically, the alignment starts with coarse steps and reduces  
 426 the step size later, for instance (Liu et al., 2024, Section 3.1)  
 427 for camera assembly. We have distilled the common principles into a synthetic logging policy called  
 428 *coordinate walk*,  $\pi_{cw,l}$  that follows a structured coordinate walk with step size  $l$ . This allows us  
 429 to control the level of expertise of the logging policy and thus the quality of the collected data.  
 430 Our synthetic position policy knows the location of  $s_W$ , but can only reach it via a path that is  
 431 suboptimal in both, number of steps and direction. More precisely, it sequentially moves along  
 432 individual coordinates of the positions  $s \in \mathcal{P} \subset \mathbb{R}^m$  by choosing actions  $a \in \mathcal{A}$  along unit vectors  
 433 until  $s_i$  matches  $(s_W)_i$ . Once a dimension is traversed, the policy cycles to the next coordinate and  
 434 continues this procedure, thereby producing a structured, axis-aligned walk toward the optimum.  
 435

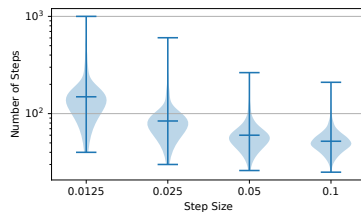


Figure 5: Expertness of  $\pi_{cw,l}$ .

If all dimensions have been optimized, the step size  $l$  is halved. By varying the initial step size, the expertness of the logging policy can be adjusted (see Figure 5). Figure 9 shows trajectories of the coordinate walk executed under different movement distortions. To model realistic hand-overs between logging policies and augmentors, we assume the internal state of the policy, i.e. the current step size  $l$  and dimensions already optimized, is reset to the initial values once the policy is reset. To not make our mathematical framework introduced in Section 3 too specific for these types of resets, we assume stateless policies there. For most states,  $V^{\pi_{l_2}}(s, W) \geq V^{\pi_{l_1}}(s, W)$  for two step sizes  $l_1 < l_2$  holds true and thus Theorem 3.4 still hold in this specific application. In Section B.2, a detailed discussion on the contraction-property and LPE of  $\pi_{cw,l}$  is given.

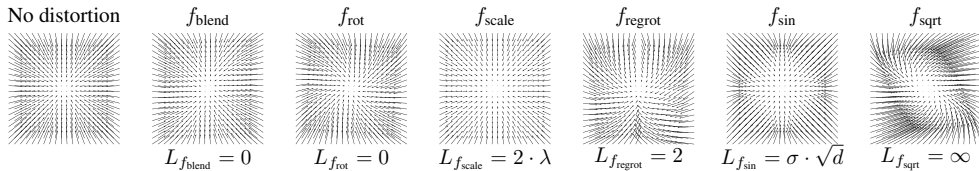


Figure 6: Movement distortions used when applying actions  $\text{clip}_\lambda(s_W - s)$ .

## 5.2 RESULTS

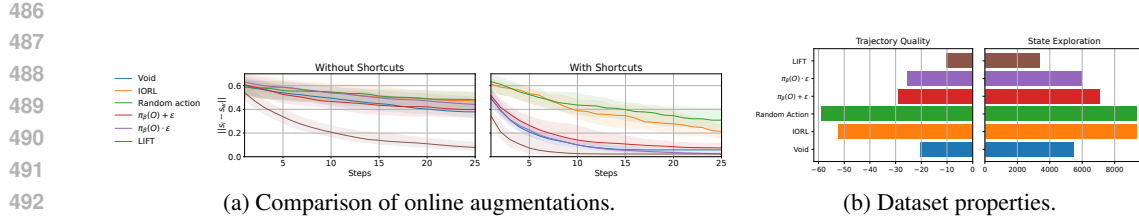
Our approach from Section 4 gives rise to essential two algorithms. First, a purely offline one that takes a static dataset collected from some logging policy and trains an offline RL algorithm with shortcut augmentations. In our experiments, we use CQL and denote this algorithm as CQL-SC. Second, an iterative offline RL algorithm that collects data with an augmented logging policy where CQL is trained on the collected data, called LIFT. If the subsequently trained CQL also uses shortcuts, we denote this algorithm as LIFT-SC. By default, we use Algorithm 2 with  $p = 0.6$ , limit augmentations per trajectory to 20. A detailed hyperparameter analysis is given in Section D.1.

First, we want to analyze the effect of different augmentations while collecting data and the effect of using shortcuts in the CQL training afterward. Beside naive augmentations as adding gaussian noise  $\pi_\beta(o) + \epsilon$  or randomly scaling actions  $\pi_\beta(o) \cdot \epsilon$  with  $\epsilon = 2 \cdot \exp(\eta), \eta \sim \mathcal{N}(0, \sigma)$ , we also use uniformly sampled actions from  $\mathcal{A}$  and IORL-like augmentations based on an uncertainty model as in Zhang et al. (2023). We run these experiments in  $(\mathcal{O}_{PO}, f_{blend})$  with step size 0.025 in  $d = 5$  dimensions, collected 3 independent datasets consisting of 100 trajectories each and trained 3 independent CQL policies on each of them. The LIFT augmentor is trained once after 50 trajectories. The averaged convergences to  $s_W$  of the CQL policies, each evaluated on 20 randomly drawn contexts are shown in Figure 7a. Here, we see that, independently of shortcuts are used in the training afterward, the best CQL policies can be obtained when trained on the data collected with LIFT. Moreover, we see that when training takes place with shortcuts, every policy can be improved. This finding is underpinned when computing the dataset characteristics introduced in Schweighofer et al. (2022) shown in Figure 7b. LIFT creates trajectories having the highest average returns reproducing findings in Schweighofer et al. (2022) that this correlates with CQL performance. On the other hand, LIFT does not explore the space as good as other methods, showing a clear differentiation to IORL that has been explicitly designed to explore well. However, high exploration comes at the price of an impeded hand-off back to the logging policy, leading to low trajectory qualities for IORL and random actions.

In our second type of experiments, we want to evaluate how our methods compare under different movement distortions and observation types. In  $\mathcal{O}_{PO}$ , algorithms collect a total of  $n = 100$  and  $n = 500$  trajectories for  $d = 2$  and  $d = 5$  respectively, where the LIFT augmentor is trained once after 50 and 100 collected trajectories respectively. In  $\mathcal{O}_{LP}$ , we collect 500 trajectories and LIFT is trained once after 100 episodes. In  $\mathcal{O}_{LT}$ , we collect only 100 trajectories and LIFT is trained once after 50 collected trajectories. Here, we additionally compare to SAC Haarnoja et al. (2018) trained

$\pi_{cw,l}$	.0125	.025	.05	.1
$f_{blend}$	•	•	•	•
$f_{scale}$	•	•	•	•
$f_{rot}$	•	•	•	•
$f_{regrat}$	•			
$f_{sin}$	•	•	•	•
$f_{sqrt}$		•	•	•

Table 1: Cases where LIFT-SC outperforms SAC baseline in  $\mathcal{O}_{PO}$ ,  $d = 5$ .

Figure 7: Experiments in  $(\mathcal{O}_{PO}, f_{blend})$  with step size  $l = 0.025$  with  $d = 5$ .

with a mixture of offline and online data as done in warm-start RL that is restricted to the same number of trajectories as in our offline datasets. Specifically, in a scenario with  $n$  many episodes, the replay buffer of SAC is initialized with the same number of trajectories collected by the logging policy the LIFT augmentor obtains in training, e.g.  $m = 50$  for  $\mathcal{O}_{LT}$ . Moreover, we also compare to diffusion-based techniques, like GTA Lee et al. (2024) that generate synthetic transitions and Diffusion-QL (DQL) Wang et al. (2023) that learns a diffusion-based policy. Figure 8 presents selected comparisons across the multiple scenarios and all comparisons can be found in Section D. In all tested environments, we see that CQL policies trained offline on data from LIFT have better performance than these trained on unaugmented data from the logging policy. This effect fades a bit when adding shortcuts to the subsequent offline training: In most scenarios, the performance of LIFT-SC is better or equal than CQL-SC. This is, for instance, not the case in when using image data from  $\mathcal{O}_{LP}$ , where CQL training on data obtained from LIFT-SC showed high variance. Studying the effect of shortcuts in isolation, CQL-SC consistently outperforms CQL and LIFT-SC consistently outperforms LIFT, making LIFT-SC the best of our methods. Comparing LIFT-SC to the SAC with offline data, we see a clear picture: SAC stays ahead in all low-dimensional cases for  $\mathcal{O}_{PO}$ , and LIFT-SC outperforms SAC almost consistently over all movement dynamics and expert-levels of the logging policy in  $\mathcal{O}_{PO}$  for  $d = 5$  (see Table 1), as well as in image-based scenarios. Interestingly, for  $f_{regrot}$  where the contraction property is violated, augmentations with shortcut fail where in  $f_{sqrt}$ , where LPE does not hold, augmentations still help but the advantage over SAC is almost negligible.

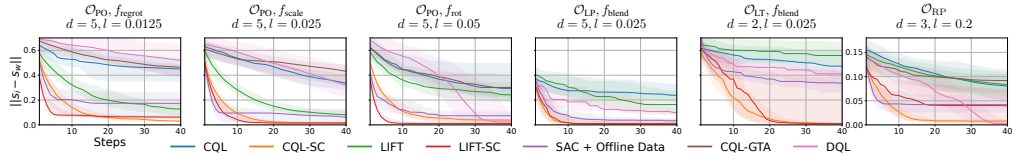


Figure 8: Comparisons of our methods under various distortions and observation types.

## 6 DISCUSSION

We demonstrate that shortcut augmentations can consistently improve the effectiveness of offline RL in active positioning problems in both, theoretical and experimental validations. In particular, we find that augmentations provide the largest gains in complex scenarios with higher action dimensionality or partial observability, where plain offline RL often fails. This suggests that exploiting task structure to expand data coverage is a promising alternative to relying solely on behavior regularization. Compared to warm-start RL, LIFT offers a more data-efficient way to leverage suboptimal expert routines: by selectively taking shortcuts suggested by an off-policy learner, we improve dataset quality without requiring extensive online fine-tuning. Nevertheless, our approach has limitations. Shortcut validity depends on assumptions about the distortion function and value function regularity, which may not hold in all real-world positioning systems. Moreover, our experiments are limited to semi-realistic simulators; future work should validate these methods on physical platforms, especially in robotic alignment tasks. Another open question is how to combine shortcut augmentation with model-based methods or world models to further improve sample efficiency. We believe that the principles underlying LIFT are broadly applicable beyond active positioning tasks where expert routines exist but are suboptimal. We hope this work encourages a more systematic treatment of data augmentation strategies for offline RL in structured industrial tasks.

540

## ETHICS STATEMENT

541

542 This work investigates RL methods for active positioning problems, with a particular focus on data  
 543 augmentation for improving offline policy learning. Our experiments are conducted exclusively in  
 544 simulated environments and do not involve human subjects, personal data, or sensitive information.  
 545 The proposed methods are designed for applications such as optical alignment and robotic  
 546 positioning in industrial settings, where potential impacts include increased energy efficiency and  
 547 reduced material waste through more accurate and reliable automation. We do not anticipate any di-  
 548 rect negative societal consequences of this research. However, as with any advancement in machine  
 549 learning for automation, care should be taken to ensure that these methods are deployed in ways that  
 complement human expertise and respect workplace safety standards.

550

551

## REPRODUCIBILITY STATEMENT

552

553 All proofs for the theoretical results in Section 3 are provided in Section A. The mathematical prop-  
 554 erties of the movement distortions used in our experiments in Section 5 are given in Section B.  
 555 Further implementation details and results of all benchmarks of our experimental validation from  
 556 Section 5, can be found in Section D. The implementations of our experiments are among the sup-  
 557 plemental material of this submission and will be made available on GitHub upon acceptance.

558

559

## LLM STATEMENT

560

561 Large language models (LLMs) were used to refine the manuscript’s language, particularly to  
 562 streamline paragraphs, improve reading flow and grammar using original drafts as input, streamlin-  
 563 ing and refining mathematical expressions, and helped to address LaTeX-specific issues. Moreover,  
 564 they provided to refine the mathematical definitions of some movement distortions and polishing  
 565 a lengthy proof via induction for Proposition 3.3. They also assisted in summarizing related work  
 566 and provided guidance on the experimental code (e.g., refactoring and debugging hints). All outputs  
 567 were reviewed and edited by the authors, who take full responsibility for the final content.

568

569

## REFERENCES

570

571 Qichang An, Xiaoxia Wu, Xudong Lin, Jianli Wang, Tao Chen, Jingxu Zhang, Hongwen Li, Haifeng  
 572 Cao, Jing Tang, Ningxin Guo, and Hongchao Zhao. Alignment of decam-like large survey  
 573 telescope for real-time active optics and error analysis. *Optics Communications*, 484:126685,  
 2021. ISSN 0030-4018. doi: <https://doi.org/10.1016/j.optcom.2020.126685>. URL <https://www.sciencedirect.com/science/article/pii/S0030401820311032>.

574

575 Marcin Andrychowicz, Filip Wolski, Alex Ray, Jonas Schneider, Rachel Fong, Peter Welinder,  
 576 Bob McGrew, Josh Tobin, OpenAI Pieter Abbeel, and Wojciech Zaremba. Hindsight experi-  
 577 ence replay. In I. Guyon, U. Von Luxburg, S. Bengio, H. Wallach, R. Fergus, S. Vishwanathan,  
 578 and R. Garnett (eds.), *Advances in Neural Information Processing Systems*, volume 30. Cur-  
 579 ran Associates, Inc., 2017. URL [https://proceedings.neurips.cc/paper\\_files/paper/2017/file/453fadbd8a1a3af50a9df899537b5-Paper.pdf](https://proceedings.neurips.cc/paper_files/paper/2017/file/453fadbd8a1a3af50a9df899537b5-Paper.pdf).

580

581

Philip J. Ball, Laura Smith, Ilya Kostrikov, and Sergey Levine. Efficient online reinforcement learn-  
 582 ing with offline data. In Andreas Krause, Emma Brunskill, Kyunghyun Cho, Barbara Engelhardt,  
 583 Sivan Sabato, and Jonathan Scarlett (eds.), *Proceedings of the 40th International Conference on  
 584 Machine Learning*, volume 202 of *Proceedings of Machine Learning Research*, pp. 1577–1594.  
 585 PMLR, 23–29 Jul 2023. URL <https://proceedings.mlr.press/v202/ball23a.html>.

586

587

K. Bräuniger, D. Stickler, D. Winters, C. Volmer, M. Jahn, and S. Krey. Automated assembly of  
 588 camera modules using active alignment with up to six degrees of freedom. In Yakov G. Soskind  
 589 and Craig Olson (eds.), *Photonic Instrumentation Engineering*, volume 8992, pp. 89920F. In-  
 590 ternational Society for Optics and Photonics, SPIE, 2014. doi: 10.1117/12.2041754. URL  
 591 <https://doi.org/10.1117/12.2041754>.

592

593

Matthias Burkhardt, Tobias Schmähling, Pascal Stegmann, Michael Layh, and Tobias Windisch.  
 594 Active alignments of lens systems with reinforcement learning, 2025. URL <https://arxiv.org/abs/2503.02075>.

594 Nicholas E. Corrado, Yuxiao Qu, John U. Balis, Adam Labiosa, and Josiah P. Hanna. Guided data  
 595 augmentation for offline reinforcement learning and imitation learning. *Reinforcement Learning*  
 596 *Conference (RLC)*, 2024.

597 Justin Fu, Aviral Kumar, Ofir Nachum, George Tucker, and Sergey Levine. D4rl: Datasets for deep  
 598 data-driven reinforcement learning, 2021. URL <https://arxiv.org/abs/2004.07219>.

600 Scott Fujimoto and Shixiang Gu. A minimalist approach to offline reinforcement learning. In  
 601 A. Beygelzimer, Y. Dauphin, P. Liang, and J. Wortman Vaughan (eds.), *Advances in Neural*  
 602 *Information Processing Systems*, 2021. URL <https://openreview.net/forum?id=Q32U7dzWXpc>.

604 Scott Fujimoto, David Meger, and Doina Precup. Off-policy deep reinforcement learning without  
 605 exploration. In *International Conference on Machine Learning*, pp. 2052–2062, 2019.

607 Juan L. Gamella, Jonas Peters, and Peter B”uhlmann. Causal chambers as a real-world  
 608 physical testbed for AI methodology. *Nature Machine Intelligence*, 2025. doi: 10.1038/  
 609 s42256-024-00964-x.

610 Tuomas Haarnoja, Aurick Zhou, Pieter Abbeel, and Sergey Levine. Soft actor-critic: Off-policy  
 611 maximum entropy deep reinforcement learning with a stochastic actor. In Jennifer Dy and An-  
 612 dreas Krause (eds.), *Proceedings of the 35th International Conference on Machine Learning*,  
 613 volume 80 of *Proceedings of Machine Learning Research*, pp. 1861–1870. PMLR, 10–15 Jul  
 614 2018. URL <https://proceedings.mlr.press/v80/haarnoja18b.html>.

616 Zhang-Wei Hong, Pulkit Agrawal, Remi Tachet des Combes, and Romain Laroche. Harnessing  
 617 mixed offline reinforcement learning datasets via trajectory weighting. In *The Eleventh Interna-*  
 618 *tional Conference on Learning Representations*, 2023. URL [https://openreview.net/forum?id=OhUAb1g27z](https://openreview.net/</a><br/>
  619 <a href=).

620 Ilya Kostrikov, Ashvin Nair, and Sergey Levine. Offline reinforcement learning with implicit q-  
 621 learning. In *International Conference on Learning Representations*, 2022. URL [https://openreview.net/forum?id=68n2s9ZJWF8](https://openreview.net/</a><br/>
  622 <a href=).

624 Aviral Kumar, Aurick Zhou, George Tucker, and Sergey Levine. Conservative q-learning for of-  
 625 fline reinforcement learning. In H. Larochelle, M. Ranzato, R. Hadsell, M.F. Balcan, and H. Lin  
 626 (eds.), *Advances in Neural Information Processing Systems*, volume 33, pp. 1179–1191. Cur-  
 627 ran Associates, Inc., 2020. URL [paper/2020/file/0d2b2061826a5df3221116a5085a6052-Paper.pdf](https://proceedings.neurips.cc/paper_files/</a><br/>
  628 <a href=).

629 Aviral Kumar, Joey Hong, Anikait Singh, and Sergey Levine. When should we prefer offline rein-  
 630 forcement learning over behavioral cloning? In *International Conference on Learning Represen-*  
 631 *tations*, 2022.

632 Patrik Langehanenberg, Josef Heinisch, Chrisitan Wilde, Felix Hahne, and Bernd Lüerß. Strategies  
 633 for active alignment of lenses. In Julie L. Bentley and Sebastian Stoebenau (eds.), *Optifab 2015*,  
 634 volume 9633, pp. 963314. International Society for Optics and Photonics, SPIE, 2015. doi: 10.  
 635 1117/12.2195936. URL <https://doi.org/10.1117/12.2195936>.

637 Misha Laskin, Kimin Lee, Adam Stooke, Lerrel Pinto, Pieter Abbeel, and Aravind Srinivas.  
 638 Reinforcement learning with augmented data. In H. Larochelle, M. Ranzato,  
 639 R. Hadsell, M.F. Balcan, and H. Lin (eds.), *Advances in Neural Information Pro-*  
 640 *cessing Systems*, volume 33, pp. 19884–19895. Curran Associates, Inc., 2020. URL  
 641 [https://proceedings.neurips.cc/paper\\_files/paper/2020/file/e615c82aba461681ade82da38004a-Paper.pdf](https://proceedings.neurips.cc/paper_files/paper/2020/file/e615c82aba461681ade82da38004a-Paper.pdf).

643 Jaewoo Lee, Sujin Yun, Taeyoung Yun, and Jinkyoo Park. Gta: Generative trajectory augmen-  
 644 tation with guidance for offline reinforcement learning. In A. Globerson, L. Mackey, D. Bel-  
 645 grave, A. Fan, U. Paquet, J. Tomczak, and C. Zhang (eds.), *Advances in Neural Information Pro-*  
 646 *cessing Systems*, volume 37, pp. 56766–56801. Curran Associates, Inc., 2024. doi: 10.52202/  
 647 079017-1808. URL [https://proceedings.neurips.cc/paper\\_files/paper/2024/file/67ea314d1df751bbf99ab664ae3049a5-Paper-Conference.pdf](https://proceedings.neurips.cc/paper_files/paper/2024/file/67ea314d1df751bbf99ab664ae3049a5-Paper-Conference.pdf).

648 Sergey Levine, Aviral Kumar, George Tucker, and Justin Fu. Offline reinforcement learning: Tu-  
 649 torial, review, and perspectives on open problems, 2020. URL <https://arxiv.org/abs/2005.01643>.

650

651 Guanghe Li, Yixiang Shan, Zhengbang Zhu, Ting Long, and Weinan Zhang. DiffStitch: Boosting  
 652 offline reinforcement learning with diffusion-based trajectory stitching. In Ruslan Salakhutdinov,  
 653 Zico Kolter, Katherine Heller, Adrian Weller, Nuria Oliver, Jonathan Scarlett, and Felix  
 654 Berkenkamp (eds.), *Proceedings of the 41st International Conference on Machine Learning*, vol-  
 655 ume 235 of *Proceedings of Machine Learning Research*, pp. 28597–28609. PMLR, 21–27 Jul  
 656 2024. URL <https://proceedings.mlr.press/v235/li24bf.html>.

657

658 Haibin Liu, Wenyong Li, Shaohua Gao, Qi Jiang, Lei Sun, Benhao Zhang, Liefeng Zhao, Jiahuang  
 659 Zhang, and Kaiwei Wang. Application of deep learning in active alignment leads to high-  
 660 efficiency and accurate camera lens assembly. *Opt. Express*, 32(25):43834–43849, Dec 2024.  
 661 doi: 10.1364/OE.537241. URL <https://opg.optica.org/oe/abstract.cfm?URI=oe-32-25-43834>.

662

663 Cong Lu, Philip Ball, Yee Whye Teh, and Jack Parker-Holder. Synthetic experience replay. In  
 664 A. Oh, T. Naumann, A. Globerson, K. Saenko, M. Hardt, and S. Levine (eds.), *Advances in  
 665 Neural Information Processing Systems*, volume 36, pp. 46323–46344. Curran Associates, Inc.,  
 666 2023. URL [https://proceedings.neurips.cc/paper\\_files/paper/2023/file/911fc798523e7d4c2e9587129fcf88fc-Paper-Conference.pdf](https://proceedings.neurips.cc/paper_files/paper/2023/file/911fc798523e7d4c2e9587129fcf88fc-Paper-Conference.pdf).

667

668 Aditya Modi, Nan Jiang, Satinder Singh, and Ambuj Tewari. Markov decision processes with contin-  
 669 uous side information. In Firdaus Janoos, Mehryar Mohri, and Karthik Sridharan (eds.), *Proceed-  
 670 ings of Algorithmic Learning Theory*, volume 83 of *Proceedings of Machine Learning Research*,  
 671 pp. 597–618. PMLR, 07–09 Apr 2018. URL <https://proceedings.mlr.press/v83/modi18a.html>.

672

673

674 Ashvin Nair, Bob McGrew, Marcin Andrychowicz, Wojciech Zaremba, and Pieter Abbeel. Over-  
 675 coming exploration in reinforcement learning with demonstrations. In *2018 IEEE International  
 676 Conference on Robotics and Automation (ICRA)*, pp. 6292–6299, 2018. doi: 10.1109/ICRA.2018.  
 677 8463162.

678

679 Robert E. Parks. Alignment of optical systems. In *International Optical Design*, pp. MB4. Op-  
 680 tica Publishing Group, 2006. doi: 10.1364/IODC.2006.MB4. URL <https://opg.optica.org/abstract.cfm?URI=IODC-2006-MB4>.

681

682 Silviu Pitis, Elliot Creager, and Animesh Garg. Counterfactual data augmentation using lo-  
 683 cally factored dynamics. In H. Larochelle, M. Ranzato, R. Hadsell, M.F. Balcan, and H. Lin  
 684 (eds.), *Advances in Neural Information Processing Systems*, volume 33, pp. 3976–3990. Cur-  
 685 ran Associates, Inc., 2020. URL [https://proceedings.neurips.cc/paper\\_files/paper/2020/file/294e09f267683c7ddc6cc5134a7e68a8-Paper.pdf](https://proceedings.neurips.cc/paper_files/paper/2020/file/294e09f267683c7ddc6cc5134a7e68a8-Paper.pdf).

686

687 Matthias Plappert, Marcin Andrychowicz, Alex Ray, Bob McGrew, Bowen Baker, Glenn Powell,  
 688 Jonas Schneider, Josh Tobin, Maciek Chociej, Peter Welinder, Vikash Kumar, and Wojciech  
 689 Zaremba. Multi-goal reinforcement learning: Challenging robotics environments and request  
 690 for research, 2018. URL <https://arxiv.org/abs/1802.09464>.

691

692 Ildar Rakhmatulin, Donald Risbridger, Richard M. Carter, M.J. Daniel Esser, and Mustafa Suphi  
 693 Erden. A review of automation of laser optics alignment with a focus on machine learning  
 694 applications. *Optics and Lasers in Engineering*, 173:107923, 2024. ISSN 0143-8166. doi:  
 695 <https://doi.org/10.1016/j.optlaseng.2023.107923>. URL <https://www.sciencedirect.com/science/article/pii/S0143816623004529>.

696

697 Kajetan Schweighofer, Marius-constantin Dinu, Andreas Radler, Markus Hofmarcher, Vi-  
 698 hang Prakash Patil, Angela Bitto-nemling, Hamid Eghbal-zadeh, and Sepp Hochreiter. A dataset  
 699 perspective on offline reinforcement learning. In Sarath Chandar, Razvan Pascanu, and Doina  
 700 Precup (eds.), *Proceedings of The 1st Conference on Lifelong Learning Agents*, volume 199  
 701 of *Proceedings of Machine Learning Research*, pp. 470–517. PMLR, 22–24 Aug 2022. URL  
<https://proceedings.mlr.press/v199/schweighofer22a.html>.

702 Takuma Seno and Michita Imai. d3rlpy: An offline deep reinforcement learning library. *Journal of*  
 703 *Machine Learning Research*, 23(315):1–20, 2022. URL <http://jmlr.org/papers/v23/22-0017.html>.  
 704

705 Samarth Sinha, Ajay Mandlekar, and Animesh Garg. S4rl: Surprisingly simple self-supervision  
 706 for offline reinforcement learning in robotics. In Aleksandra Faust, David Hsu, and Ger-  
 707 hard Neumann (eds.), *Proceedings of the 5th Conference on Robot Learning*, volume 164 of  
 708 *Proceedings of Machine Learning Research*, pp. 907–917. PMLR, 08–11 Nov 2022. URL  
 709 <https://proceedings.mlr.press/v164/sinha22a.html>.  
 710

711 Richard S. Sutton and Andrew G. Barto. *Reinforcement Learning: An Introduction*. The MIT Press,  
 712 second edition, 2018.  
 713

714 Denis Tarasov, Vladislav Kurenkov, Alexander Nikulin, and Sergey Kolesnikov. Revisiting the  
 715 minimalist approach to offline reinforcement learning. In *Thirty-seventh Conference on Neu-*  
 716 *ral Information Processing Systems*, 2023. URL <https://openreview.net/forum?id=vqGWs1LeEw>.  
 717

718 Robert Upton, Thomas Rimmele, and Robert Hubbard. Active optical alignment of the Advanced  
 719 Technology Solar Telescope. In Martin J. Cullum and George Z. Angeli (eds.), *Modeling, Systems*  
 720 *Engineering, and Project Management for Astronomy II*, volume 6271, pp. 62710R. International  
 721 Society for Optics and Photonics, SPIE, 2006. doi: 10.1117/12.671826. URL <https://doi.org/10.1117/12.671826>.  
 722

723 Andrew Wagenmaker, Zhiyuan Zhou, and Sergey Levine. Behavioral exploration: Learning to ex-  
 724 plore via in-context adaptation. In Aarti Singh, Maryam Fazel, Daniel Hsu, Simon Lacoste-Julien,  
 725 Felix Berkenkamp, Tegan Maharaj, Kiri Wagstaff, and Jerry Zhu (eds.), *Proceedings of the 42nd*  
 726 *International Conference on Machine Learning*, volume 267 of *Proceedings of Machine Learning*  
 727 *Research*, pp. 61885–61912. PMLR, 13–19 Jul 2025. URL <https://proceedings.mlr.press/v267/wagenmaker25a.html>.  
 728

729 Zhendong Wang, Jonathan J Hunt, and Mingyuan Zhou. Diffusion policies as an expressive policy  
 730 class for offline reinforcement learning. In *The Eleventh International Conference on Learning*  
 731 *Representations*, 2023. URL <https://openreview.net/forum?id=AHvFDPi-FA>.  
 732

733 Denis Yarats, David Brandfonbrener, Hao Liu, Michael Laskin, Pieter Abbeel, Alessandro Lazaric,  
 734 and Lerrel Pinto. Don’t change the algorithm, change the data: Exploratory data for offline  
 735 reinforcement learning. In *Generalizable Policy Learning in the Physical World Workshop at*  
 736 *International Conference on Learning Representations*, 2022.  
 737

738 Lan Zhang, Luigi Franco Tedesco, Pankaj Rajak, Youcef Zemmouri, and Hakan Brunzell. Ac-  
 739 tive learning for iterative offline reinforcement learning. In *NeurIPS 2023 Workshop on Adap-*  
 740 *tive Experimental Design and Active Learning in the Real World*, 2023. URL <https://openreview.net/forum?id=yuJEkWSkTN>.  
 741

## 742 A PROOFS FOR SECTION 3

743

744 **Lemma A.1.** *Let  $\pi$  be distance-improving, then  $(1 - \gamma)V^\pi(s, W) \geq -\|s - s_W\|$  for all  $(s, W)$ .*

745 *Proof.* Let  $(s_0, W), (s_1, W), \dots, (s_k, W)$  be a trajectory of  $\pi$  starting at  $s = s_0$ , then  
 746

$$747 V^\pi(s, W) = - \sum_{i=1}^k \gamma^{i-1} \|s_i - s_W\| \geq -\|s - s_W\| \sum_{i=0}^{k-1} \gamma^i = -\|s - s_W\| \cdot \frac{1 - \gamma^k}{1 - \gamma}$$

748 where we have used that  $\pi$  is distance improving in every step. Finally,  $(1 - \gamma)V^\pi(s, W) \geq -\|s - s_W\|(1 - \gamma^k) \geq -\|s - s_W\|$ .  $\square$   
 749

756 *Proof of Proposition 3.1.* Assume that  $\tau = (s_0, \dots, s_k)$  is the sub-trajectory of  $\pi$  starting at  $s = s_0$   
 757 and ending at  $s' = s_k$ . We prove the statement via induction on  $k$ . Note that since  $s' \neq s$ , we have  
 758  $k \geq 1$ . Let  $k = 1$ , then

$$759 \quad 760 \quad V^\pi(s, W) = -\|s_1 - s_W\| + \gamma \cdot V^\pi(s', W)$$

761 and the claim holds. Now, assume the statement holds from  $s_1$  to  $s_k = s'$ , then

$$762 \quad 763 \quad \gamma V^\pi(s', W) - V^\pi(s_1, W) \geq \|s' - s_W\|$$

764 by the induction hypothesis. Furthermore, we have

$$765 \quad \gamma V^\pi(s', W) - V^\pi(s, W) = \gamma V^\pi(s', W) - V^\pi(s_1, W) + V^\pi(s_1, W) - V^\pi(s, W) \\ 766 \quad \geq \|s' - s_W\| + V^\pi(s_1, W) - V^\pi(s, W) \\ 767 \quad = \|s' - s_W\| + V^\pi(s_1, W) - (-\|s_1 - s_W\| + \gamma V^\pi(s_1, W)) \\ 768 \quad = \|s' - s_W\| + (1 - \gamma)V^\pi(s_1, W) + \|s_1 - s_W\|$$

770 Using Lemma A.1, we have  $(1 - \gamma)V^\pi(s_1, W) + \|s_1 - s_W\| \geq 0$  and the claim follows.  $\square$   
 771

772 *Proof of Proposition 4.1.* We denote  $\pi_\beta$  simply by  $\pi$  in the following. It suffices to show that the  
 773 statement holds if augmentation only is applied at one single state  $(\tilde{s}, W)$  as we then can apply the  
 774 statement repeatedly. That is, there exists an action  $a$  that satisfies:

$$775 \quad 776 \quad \gamma \cdot V^\pi(f(\tilde{s}, a, W), W) - \|f(\tilde{s}, a, W) - s_W\| \geq V^\pi(\tilde{s}, W)$$

777 Let  $\pi_a$  be the policy that uses  $a$  at  $\tilde{s}$  and on all other states coincides with  $\pi$ . First, we show that  
 778  $J(\pi_a) \geq J(\pi)$ . It suffices to show that  $V^{\pi_a}(s) \geq V^\pi(s)$  for all  $s \in S$ . Let  $(s, W)$  be an initial  
 779 state. If the trajectory of  $\pi$  does not traverse  $\tilde{s}$ , then  $V^{\pi_a}(s) = V^\pi(s)$ . Assume differently that the  
 780 trajectory visits  $\tilde{s}$  at the  $t$ -th step. Then, the trajectory starting at  $s$  follows  $\pi$  till  $\tilde{s}$ , then chooses the  
 781 shortcut  $a$ , and then follows  $\pi$  from  $s' = f(\tilde{s}, a, W)$ . The value for this trajectory is:

$$783 \quad V^{\pi_a}(s, W) = V^\pi(s, W) - \gamma^t \cdot V^\pi(\tilde{s}, W) - \gamma^t \|s' - s_W\| + \gamma^{t+1} V^\pi(s', W).$$

784 From the assumption of  $(\tilde{s}, a)$ , we have

$$786 \quad 787 \quad \gamma^t \cdot (-V^\pi(\tilde{s}, W) - \|s' - s_W\| + \gamma \cdot V^\pi(s', W)) \geq 0$$

788 and hence  $V^{\pi_a}(s, W) \geq V^\pi(s, W)$ .  $\square$

789 *Proof of Proposition 3.2.* Since Proposition 3.1 gives that  $\gamma V^\pi(s_j, W) - V^\pi(s_i, W) \geq \|s_j - s_W\|$ ,  
 790 it is left to prove that  $f(s_i, a, W) = s_j$ . We have

$$793 \quad 794 \quad f(s_i, a, W) = s_i + W \cdot \sum_{k=i}^{j-1} a_i = s_i + W \cdot a_i + W \cdot a_{i+1} + \dots + W \cdot a_{j-1}.$$

795 Let  $s_{i+1}, \dots, s_{j-2}$  be the intermediate states, i.e.  $s_k = f(s_{k-1}, a_{k-1}, W)$ , then replacing  $s_k =$   
 796  $s_{k-1} + W \cdot a_{k-1}$  in the equation above from  $k = i$  to  $k = j - 1$  gives the claim.  $\square$

797 *Proof of Proposition 3.3.* Let  $a_0, \dots, a_{k-1}$  a chain of actions and set  $A = \sum_{i=0}^{k-1} a_i$ ,  $(s_0, W)$  an  
 798 initial state and set  $s_i = f(s_{i-1}, a_{i-1}, W)$ . Recursively unraveling the definition of  $f$  yields

$$801 \quad 802 \quad s_k = s_0 + \sum_{i=0}^{k-1} g(s_i, W) \cdot a_i$$

803 and consequently

$$805 \quad 806 \quad f(s_0, A, W) - s_k = g(s_0, W) \sum_{i=0}^{k-1} a_i - \sum_{i=0}^{k-1} g(s_i, W) a_i \\ 807 \\ 808 \quad = \sum_{i=0}^{k-1} (g(s_0, W) - g(s_i, W)) a_i.$$

810 Taking norms and using the induced matrix norm on  $\mathbb{R}^{m \times d}$  gives  
 811

$$812 \quad \|f(s_0, A, W) - s_k\| \leq \sum_{i=0}^{k-1} \|g(s_0, W) - g(s_i, W)\| \cdot \|a_i\|. \\ 813 \\ 814$$

815 By the assumption on  $g$ , we have

$$816 \quad \|g(s_0, W) - g(s_i, W)\| \leq \|g(s_0, W)\| + \|g(s_i, W)\| \leq 2 \cdot \sup_{\mathcal{S} \times \mathcal{W}} \|g\| \\ 817$$

818 independently of the actions for all  $i$  and the claim follows.  $\square$   
 819

820 *Proof of Theorem 3.4.* For brevity, we omit  $W$  in the notation of the value function. We have to  
 821 show that  $\gamma V^\pi(f(s_i, a, W)) - V^\pi(s_i) \geq \|f(s_i, a, W) - s_W\|$ . Because  $f$  has linear-placement  
 822 errors, it follows directly from Definition 3.2 that  $\|f(s_i, a, W) - s_j\| \leq L_f \cdot \sum_{k=i}^{j-1} \|a_k\|$  and thus  
 823

$$824 \quad \|f(s_i, a, W) - s_W\| = \|f(s_i, a, W) - s_j + s_j - s_W\| \leq L_f \cdot \sum_{k=i}^{j-1} \|a_k\| + \|s_j - s_W\|. \\ 825 \\ 826$$

827 On the other hand, using the Lipschitz continuity of  $V^\pi$ , we get

$$828 \quad \gamma V^\pi(f(s_i, a, W)) - V^\pi(s_i) \geq \gamma \cdot (V^\pi(s_j) - L_V \cdot \|f(s_i, a, W) - s_j\|) - V^\pi(s_i) \\ 829 \\ 830 \geq \gamma \cdot V^\pi(s_j) - V^\pi(s_i) - \gamma \cdot L_V \cdot L_f \cdot \sum_{k=i}^{j-1} \|a_k\| \\ 831 \\ 832$$

833 Now, as the inequality from the theorem statement holds, we have

$$834 \quad \gamma \cdot V^\pi(s_j) - V^\pi(s_i) \geq (\gamma \cdot L_V + 1) \cdot L_f \cdot \sum_{k=i}^{j-1} \|a_k\| + \|s_j - s_W\| \\ 835 \\ 836$$

837 and plugging this into the upper equation gives the claim.  $\square$   
 838

839 **Proposition A.2.** *Let  $\pi$  be an  $f$ -contraction. Then  $V^\pi$  is  $\frac{1}{1-\gamma}$ -Lipschitz continuous in the states.*  
 840

841 *Proof.* Define  $L = \frac{1}{1-\gamma}$  and let  $(s, W)$  and  $(s', W)$  be two states. We prove via induction over the  
 842 combined number of steps  $k$  needed to reach the optimality region around  $s_W$  starting at  $s$  and  $s'$   
 843 that

$$844 \quad |V^\pi(s, W) - V^\pi(s', W)| \leq L \cdot \|s - s'\|.$$

845 If  $k = 0$ , then  $s$  and  $s'$  are both within the optimality region, i.e.  $\|s - s_W\| \leq \theta$  and  $\|s' - s_W\| \leq \theta$ , then  $V^\pi(s, W) = V^\pi(s', W) = 0$  and the claim holds. Now, let  $o = O(s, W)$  and  
 846  $o' = O(s', W)$  be the observations at  $s$  and  $s'$  and  $s_1 = f(s, \pi(o), W)$  and  $s'_1 = f(s', \pi(o'), W)$   
 847 be the next states after one step of  $\pi$ . Particularly, the induction hypothesis holds for  $s_1$  and  $s'_1$ ,  
 848 i.e.  $|V^\pi(s_1, W) - V^\pi(s'_1, W)| \leq L \cdot \|s_1 - s'_1\|$ . Since  $V^\pi(s) = -\|s_1 - s_W\| + \gamma V^\pi(s_1, W)$  and  
 849  $V^\pi(s') = -\|s'_1 - s_W\| + \gamma V^\pi(s'_1, W)$ , we have  
 850

$$851 \quad |V^\pi(s) - V^\pi(s')| = |\gamma \cdot V^\pi(s_1, W) - \gamma \cdot V^\pi(s'_1, W) - \|s_1 - s_W\| + \|s'_1 - s_W\|| \\ 852 \\ 853 \leq \gamma \cdot |V^\pi(s_1, W) - V^\pi(s'_1, W)| + \|\|s_1 - s_W\| - \|s'_1 - s_W\|\| \\ 854 \\ 855 \leq \gamma \cdot L \cdot \|s_1 - s'_1\| + \|s_1 - s'_1\| \\ 856 \\ 857 \leq (\gamma \cdot L + 1) \cdot \|s_1 - s'_1\| \\ 858 \\ 859 = L \cdot \|s_1 - s'_1\|$$

860 where the last equation is due to  $L = \frac{1}{1-\gamma}$ . Finally, because  $\pi$  is an  $f$ -contraction, we have  $\|s_1 - s'_1\| = \|f(s, \pi(o), W) - f(s', \pi(o'), W)\| \leq \|s - s'\|$  and the claim follows.  $\square$   
 861

862 *Proof of Corollary 3.5.* Because  $\pi$  is an  $f$ -contraction,  $V^\pi$  is  $\frac{1}{1-\gamma}$ -Lipschitz continuous by Propo-  
 863 sition A.2. Plugging  $L_V = \frac{1}{1-\gamma}$  into Theorem 3.4 gives the claim.  $\square$

---

## 864 B MOVEMENT DISTORTION FUNCTIONS

866 In this section, we formally define the different movement distortions  $f$  we consider in our experiments.  
 867 The first set of distortions are linear distortions of the form  $f(s, a, W) = s + W \cdot a$  with  
 868  $W \in \mathbb{R}^{d \times d}$  a distortion matrix, more specific, we use

$$870 \quad f_{\text{blend}}(s, a, W) = s + (I_{d \times d} + W) \cdot a, \quad W \sim \mathcal{N}_{d \times d}(0, \sigma)$$

871 For  $W \in \mathbb{R}$  a scalar, let  $R_W = \begin{pmatrix} \cos(W) & -\sin(W) \\ \sin(W) & \cos(W) \end{pmatrix}$  be a two-dimensional rotation matrix. We  
 872 rise this to a high-dimensional rotation matrix where adjacent dimensions are rotated, i.e.,  
 873

$$875 \quad \text{Rot}_W = \text{diag}(R_W, \dots, R_W) \in \mathbb{R}^{d \times d}$$

876 where  $\text{diag}(A_1, \dots, A_k)$  is the block-diagonal matrix with blocks  $A_1, \dots, A_k$  on the diagonal.  
 877

$$878 \quad f_{\text{rot}}(s, a, W) = s + \text{Rot}_W \cdot a, \quad W \sim \mathcal{N}(0, \sigma)$$

880 The next distortion function is a scaling-based one which does not depend on a latent context  $W$ :  
 881

$$882 \quad f_{\text{scale}}(s, a, W) = s + \text{clip}_{C, \lambda}(\|s - s_W\|) \cdot a$$

883 with some constant  $0 < C < \lambda$  to ensure that the steps are not too small so that the optimum can be  
 884 reached in finitely many steps.  
 885

886 The next set of distortions is again a rotation-based one, but one where the rotation matrix depends  
 887 on the region. For that, we assume the position space  $\mathcal{P}$  is decomposed into  $c$ -many non-overlapping  
 888 subsets  $\mathcal{P}_1, \dots, \mathcal{P}_c$  such that  $\cup_{i=1}^c \mathcal{P}_i = \mathcal{P}$ . Then

$$889 \quad f_{\text{regrot}}(s, a, W) = s + \sum_{i=1}^c \mathbf{1}_{s \in \mathcal{P}_i} \cdot \text{Rot}_{W_i} \cdot a, \quad W \in \mathcal{N}_c(\mu, \sigma), \mu \in \mathbb{R}^c$$

892 As  $\mathcal{P}_i \cap \mathcal{P}_j = \emptyset$  for  $i \neq j$ , only one rotation matrix is active at a time, depending on the state.  
 893

894 In our experiments, we used  $c = 4$  and divided  $\mathcal{P}$  into four sets depending on in which quadrant of  
 895  $\mathbb{R}^2$  the first two dimensions reside. Moreover, we set  $\mu = (-0.3, 0.6, -0.3, 0.6)$ .  
 896

897 The next distortion is one where a non-linear offset is added which depends on both, the state and  
 898 the action:  
 899

$$f_{\text{sin}}(s, a, W) = s + a + W \cdot \sin(s) \circ \cos(s) \cdot \|a\|, \quad W \sim \mathcal{U}(0, \sigma)$$

900 where  $\sin$  and  $\cos$  are applied component-wise and  $\circ$  denote the element-wise multiplication. Fi-  
 901 nally, we consider a distortion function that does not have linear placement errors:  
 902

$$f_{\text{sqrt}}(s, a, W) = s + (I_{d \times d} + W) \cdot \sqrt{\|a\|} \cdot a, \quad W \sim \mathcal{N}_{d \times d}(0, \sigma).$$

### 904 B.1 LINEAR PLACEMENT-ERRORS

906 We begin by proving a stronger conditions, which is easier to check and implies LPE:  
 907

908 **Proposition B.1.** *Let  $f$  be a distortion function and assume there exists a constant  $L_f$  such that for  
 909 all states  $(s, W)$  and actions  $a, a' \in \mathcal{A}$*

$$910 \quad \|f(s, a + a', W) - f(f(s, a, W), a', W)\| \leq L_f \cdot \|a\|$$

911 *Then  $f$  has LPE with constant  $L_f$ .*  
 912

913 *Proof.* For  $i \in \{0, \dots, k\}$ , define the tail sums  $\tilde{a}_i := \sum_{j=i}^{k-1} a_j$  and the states  $\tilde{s}_i := f(s_i, \tilde{a}_i, W)$ .  
 914 By definition  $\tilde{s}_0 = f(s_0, a_0 + \dots + a_{k-1}, W)$  and, since  $\tilde{a}_k = 0$  and  $f(s, 0, W) = s$ , we also have  
 915  $\tilde{s}_k = s_k$ . Thus, we have to prove that  $\|\tilde{s}_0 - \tilde{s}_k\| \leq L_f \sum_{i=0}^{k-1} \|a_i\|$ . Now, for any  $i \in \{0, \dots, k-1\}$   
 916 we have  
 917

$$\|\tilde{s}_i - \tilde{s}_{i+1}\| = \|f(s_i, a_i + \tilde{a}_{i+1}, W) - f(s_{i+1}, \tilde{a}_{i+1}, W)\| \leq L_f \|a_i\|.$$



Figure 9: Trajectories of direct policy and coordinate walk in different movement dynamics.

because of the assumptions on  $f$  from the statement of the proposition. Summing these inequalities and applying the triangle inequality yields

$$\|\tilde{s}_0 - \tilde{s}_k\| \leq \sum_{i=0}^{k-1} \|\tilde{s}_i - \tilde{s}_{i+1}\| \leq L_f \sum_{i=0}^{k-1} \|a_i\|.$$

972  
973

□

974 LPE and the proposition of Proposition B.1 are not equivalent: Consider  $f(s, a) = s + \text{sign}(s) \cdot a$ .  
 975 Then its easy to show that  $f$  has linear-placement errors with  $L_f = 2$ , but it does not have the  
 976 property from Proposition B.1.

977 **Proposition B.2.** *The distortion  $f_{\text{blend}}$  has LPE with  $L_{f_{\text{blend}}} = 0$ .*

979 *Proof.* Straight-forward application of Proposition B.1. □

981 **Proposition B.3.** *The distortion  $f_{\text{rot}}$  has LPE with  $L_{f_{\text{rot}}} = 0$ .*

983 *Proof.* Straight-forward application of Proposition B.1. □

984 **Proposition B.4.** *The distortion  $f_{\text{scale}}$  has LPE with  $L_{f_{\text{scale}}} = 2 \cdot \lambda$ .*

986 *Proof.* We write  $f_{\text{scale}}(s, a, W) = s + g(s, W) \cdot a$  with  $g(s, W) = \text{clip}_{C, \lambda}(\|s - s_W\|) \cdot I_d$  with  $I_d$   
 987 the identity function of  $\mathbb{R}^{d \times d}$ . Clearly  $g$  is bounded and we have  $\sup_{S \times W} \|g\| = \lambda$  and the claim  
 988 follows by an application of Proposition 3.3. □

990 **Proposition B.5.** *The distortion  $f_{\text{regrot}}$  has LPE with  $L_{f_{\text{regrot}}} = 2$ .*

992 *Proof.* We write  $f_{\text{regrot}}(s, a, W) = s + g(s, W) \cdot a$  with  $g(s, W) = \text{Rot}_{W_i}$  whenever  $s \in \mathcal{P}_i$ , where  
 993  $\mathcal{P}_1, \dots, \mathcal{P}_c$  are the partitions of  $S$  from Section 5.1.1. For every state  $(s, W)$ ,  $g(s, W)$  is a rotation  
 994 matrix and thus  $\|g(s, W)\| = 1$  and  $g$  satisfies the the claim follows from Proposition 3.3. □

995 **Proposition B.6.** *The distortion  $f_{\text{sin}}$  has LPE with  $L_{f_{\text{sin}}} = \sqrt{d}\sigma$ .*

997 *Proof.* Let  $f_{\text{sin}}(s, a, W) = s + a + g(s) \cdot \|a\|$  with  $g(s, W) := W \cdot \sin(s) \odot \cos(s)$ . Although we  
 998 cannot apply Proposition 3.3 as  $f_{\text{sin}}$  has not the desired form, we can follow a similar strategy. First,  
 999 we observe that  $g$  is bounded:

$$1001 \quad \|g(s, W)\| = |W| \cdot \sqrt{\sum_{i=1}^d \sin(s_i)^2 \cdot \cos(s_i)^2} \leq \sigma \sqrt{d}$$

1004 because  $W \sim \mathcal{U}(0, \sigma)$ . Let  $a_0, \dots, a_{k-1}$  be a chain of actions and set  $A = \sum_{i=1}^{k-1} a_i$  and  $s_i =$   
 1005  $f(s_{i-1}, a_{i-1}, W)$ , then

$$1008 \quad f_{\text{sin}}(s_0, A, W) - s_k = A + g(s_0, W)\|A\| - \sum_{i=0}^{k-1} (a_i + g(s_i, W)\|a_i\|) = g(s_0, W)\|A\| - \sum_{i=0}^{k-1} g(s_i, W)\|a_i\|$$

1010 and thus:

$$1012 \quad \|f_{\text{sin}}(s_0, A, W) - s_k\| \leq \|g(s_0, W)\|A\| + \sum_{i=0}^{k-1} \|g(s_i, W)\|a_i\| \leq \sigma \sqrt{d} \sum_{i=0}^{k-1} \|a_i\|$$

1015 because  $\|A\| \leq \sum_{i=0}^{k-1} \|a_i\|$  by the triangle inequality. □

1017 Next, we show that  $f_{\text{sqrt}}$  is not LPE:

1018 **Proposition B.7.** *The distortion  $f_{\text{sqrt}}$  does not have LPE.*

1020 *Proof.* Let  $v \in \mathbb{R}^d$  be a unit vector and let  $a_0 = a_1 = c \cdot v$  with  $c \leq \lambda$ . Let  $(0, 0) \in \mathbb{R}^d \times \mathbb{R}^{d \times d}$   
 1021 be an initial state, then  $s_1 = f_{\text{sqrt}}(0, a_0, 0) = \sqrt{c} \cdot c \cdot v$  and  $s_2 = f_{\text{sqrt}}(s_1, a_1, 0) = 2\sqrt{c} \cdot c \cdot v$ .  
 1022 Moreover, we have  $f(s_0, a_0 + a_1, 0) = f(0, 2 \cdot c \cdot v, 0) = 2\sqrt{2c} \cdot c \cdot v$  and hence

$$1024 \quad \|f(s_0, a_0 + a_1, 0) - s_2\| = (2\sqrt{2} - 2) \cdot \sqrt{c} \cdot c.$$

1025 which cannot be bounded by  $L_f \cdot (\|a_0\| + \|a_1\|) = 2 \cdot L_f \cdot c$  for any constant  $L_f$ . □

1026  
1027

## B.2 CONTRACTIONS AND LIPSCHITZ-CONTINUITY IN REAL-WORLD APPLICATIONS

1028  
1029  
1030  
1031  
1032  
1033

We do not expect that policies and distortions from real-world applications satisfy the rigorous mathematical assumptions stated in Section 3. Pedantically, even simple modeling choices already break global smoothness: for instance, having  $\mathcal{A} = B_\lambda(0)$  with  $\mathcal{A}$  a strict subset of  $S$ , combined with an optimality region defined by a threshold  $\theta$ , induces discontinuities in the value function. The same holds for the coordinate walk policy in Section 5.1.3, where a fixed step length produces value functions with sharp discontinuities, as shown in Figure 11.

1034  
1035  
1036  
1037  
1038  
1039  
1040

Nevertheless, global mathematical rigor is not required to detect local shortcuts in real trajectories. A striking example is the coordinate walk under  $f_{\text{regrot}}$ : since different rotations apply in different regions, the policy is not an  $f$ -contraction globally, because nearby states  $s$  and  $s'$  lying in different regions  $\mathcal{P}_i$  and  $\mathcal{P}_j$  may be rotated in different directions (Figure 10a). Yet, for states within same region where the coordinate walk applies same actions, the contraction property is preserved (Figure 10b). This illustrates that shortcut identification relies less on global guarantees and more on local structure along trajectory segments.

1041  
1042  
1043  
1044  
1045  
1046

Informally speaking, it suffices that the value function does not change too abruptly for small misplacements, so that local improvements can be exploited as shortcuts. In practice, this condition is often met: physical systems typically exhibit continuity over small ranges of motion, even if discontinuities or non-contractive behavior emerge globally. Hence, while our theoretical assumptions provide clean guarantees, the underlying ideas remain applicable well beyond the idealized setting as demonstrated by our experiments in Section 5.

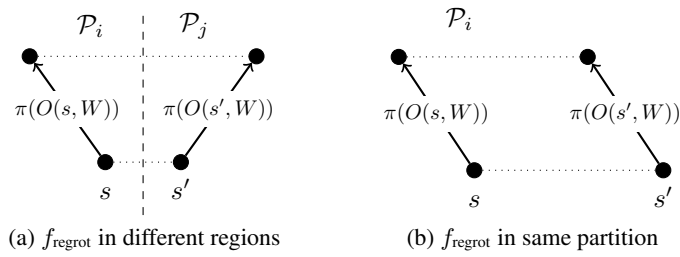
1047  
1048  
1049  
1050  
1051  
1052  
1053  
1054  
1055  
1056

Figure 10: In  $f_{\text{regrot}}$ , starting at two close-by states  $s$  and  $s'$  in different regions  $\mathcal{P}_1$  and  $\mathcal{P}_2$  can increase the distance between subsequent states as opposed rotation matrices apply.

1057  
1058  
1059  
1060  
1061  
1062  
1063  
1064  
1065  
1066  
1067  
1068  
1069  
1070  
1071  
1072  
1073  
1074  
1075  
1076  
1077  
1078  
1079

## C ADDITIONAL EXPERIMENTS IN FETCH-ENVIRONMENT

In extension to the reach experiments in Section 5 where the positional differences are directly observed, we provide in this section a proof of principle that shortcut augmentations can also benefit offline RL methods in more involved robotic environments. To this end, we consider two scenarios based on the Fetch environment Plappert et al. (2018). In the first scenario, we study a reaching task in which the robotic arm must reach a target position in 3D space. The observation is an image of the scene. We collect 100 trajectories using the coordinate walk policy described in Section 5.1.3.

In the second scenario, we consider a variant of the pick-and-place task where the robotic arm must move an object from a random initial position to a random target position. We focus solely on the positioning, i.e., the object does not need to be grasped, only touched, assuming perfect gripper

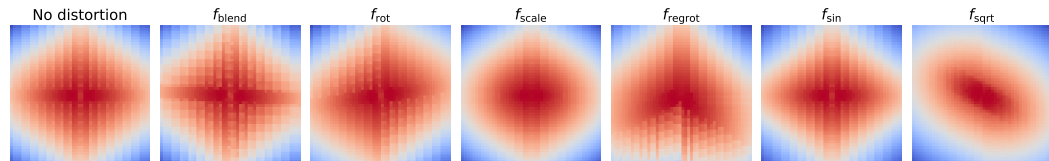


Figure 11: Value functions  $V^\pi(\cdot, W)$  of coordinate walk for a random but fixed context  $W$  each.

control. The policy used here performs two consecutive coordinate walks: one to reach the object and one to reach the target position. The observations are given by the distances from the gripper to the object and from the gripper to the target where the first distance is zeroed once solves the touching task. In this setting, we collect 1000 trajectories. On the collected datasets, we train CQL both with and without shortcuts, and the results are reported in Figure 12.

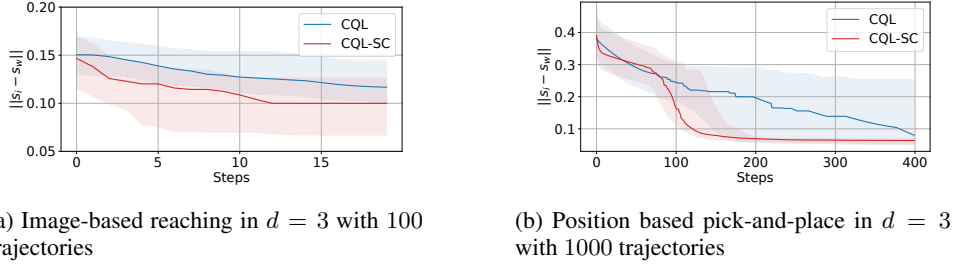


Figure 12: Experiments in the Fetch environment.

## D DETAILS FOR EXPERIMENTAL RESULTS

### D.1 HYPERPARAMETERS OF LEARNING ALGORITHMS

Parameter	Value	Parameter	Value	Parameter	Value
actor learning rate	$10^{-3}$	actor learning rate	$10^{-3}$	actor learning rate	$10^{-3}$
critic learning rate	$10^{-3}$	critic learning rate	$10^{-3}$	critic learning rate	$10^{-3}$
conservative weight	5.0	conservative weight	5.0	batch size	256
$\alpha$ -threshold	10.0	$\alpha$ -threshold	10.0	n updates per step	5
batch size	500	batch size	500	n critics	2
$\gamma$	0.99	$\gamma$	0.99	$\gamma$	0.99
$\tau$	0.005	$\tau$	0.005	$\tau$	0.005

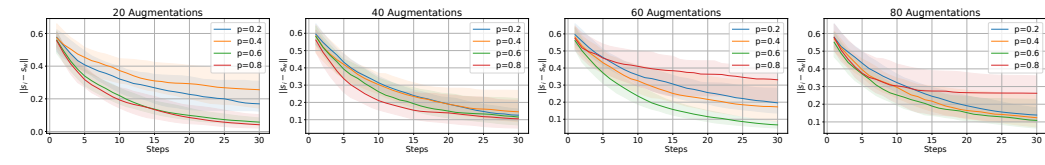
Table 2: Parameter for CQL trained on collected datasets.

Table 3: Parameter for CQL trained as LIFT augmentor.

Table 4: Parameter for SAC.

### D.2 HYPERPARAMETER STUDY OF LIFT

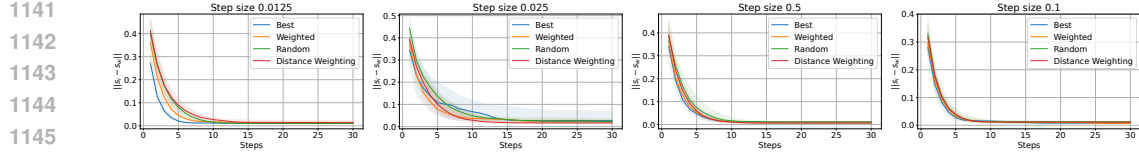
In this section, we study effects of the different hyperparameters of the shortcut computation (Algorithm 1) and LIFT (Algorithm 2). First, we study the effect of the number of augmentations per trajectory  $n$  and the probability of applying an augmentation  $p$ . The results are shown in Figure 13. One can see that as few as 20 augmentations per trajectory are sufficient to achieve a substantial improvement in performance, provided that the augmentation probability is not too low. Notably, higher probabilities correspond to augmentations being applied earlier in the trajectory. This suggests that augmentations at the beginning of a trajectory are more beneficial than those applied later.

Figure 13: Experiments in  $f_{blend}$  with step size 0.025 and different probabilities  $p$  of applying augmentations and different maximal number of augmentations per trajectory

Next, we analyse the effect of the sampling scheme of shortcuts along a trajectory. Here, we denote the sampling mechanism described in Algorithm 1 as *weighted*. Another way to sample shortcuts

1134 from the set  $S$  computed in Algorithm 1 is to use a distribution that is proportional to the inverse  
 1135 distance to the optimum, i.e.  $p(i) \sim \frac{1}{\|s_i - s_W\|}$  or to sample uniformly from  $S$ . Instead of sampling,  
 1136 one can also just use the shortcut residing within the action space that leads to the point of highest  
 1137 reward within the trajectory called *best*. The results are shown in Figure 14 for  $n = 20$  augmenta-  
 1138 tions per trajectory and  $p = 0.4$  showing that in the environments we consider, the sampling strategy  
 1139 does not have a significant effect on the performance.

1140



1146

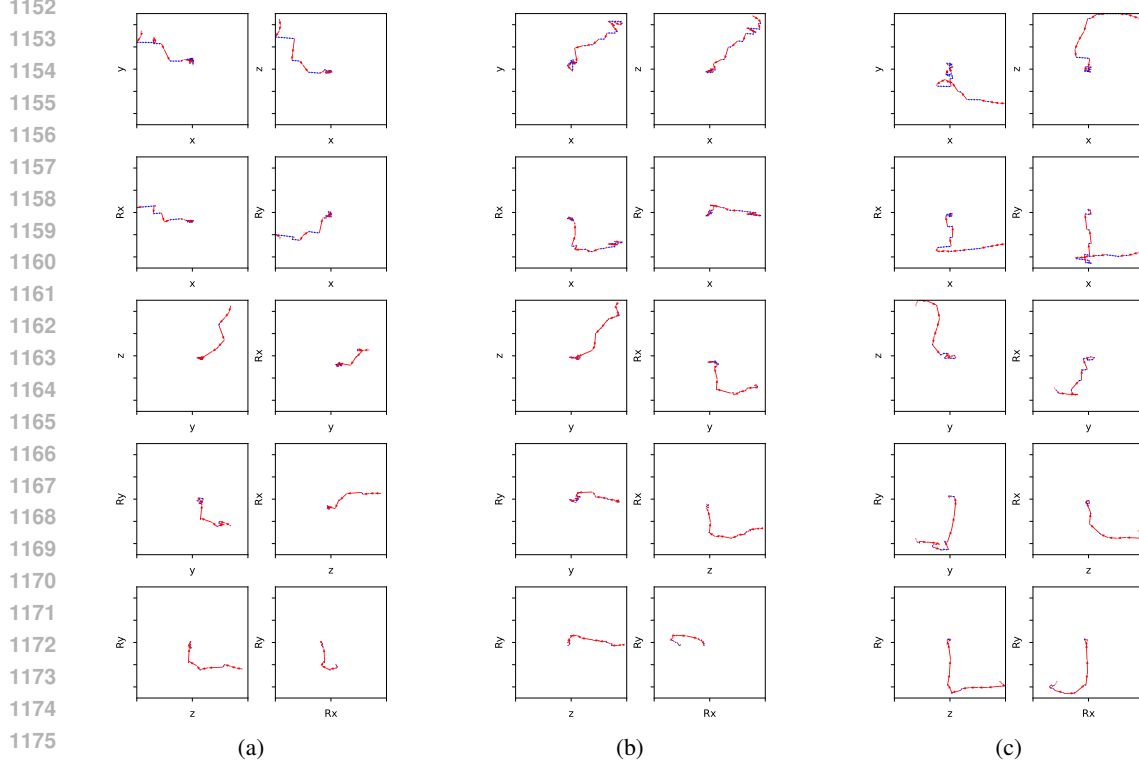
1147 Figure 14: Experiments in  $f_{\text{blend}}$  with different step size and different sampling strategies.

1148

1149 

### D.3 ADDITIONAL VISUALIZATION

1150



1176

1177 Figure 15: Augmented trajectories generated by LIFT for  $\mathcal{O}_{\text{LP}}$  in 5 dimensional hidden position  
 1178 space: Actions coming from the augmentor in red and actions from the logging policy in blue.

1179

1180

1181

1182

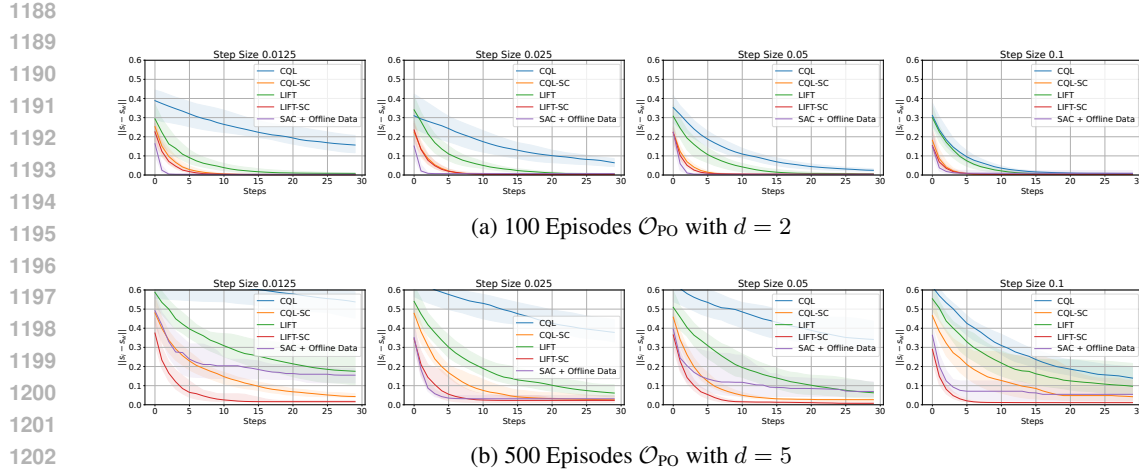
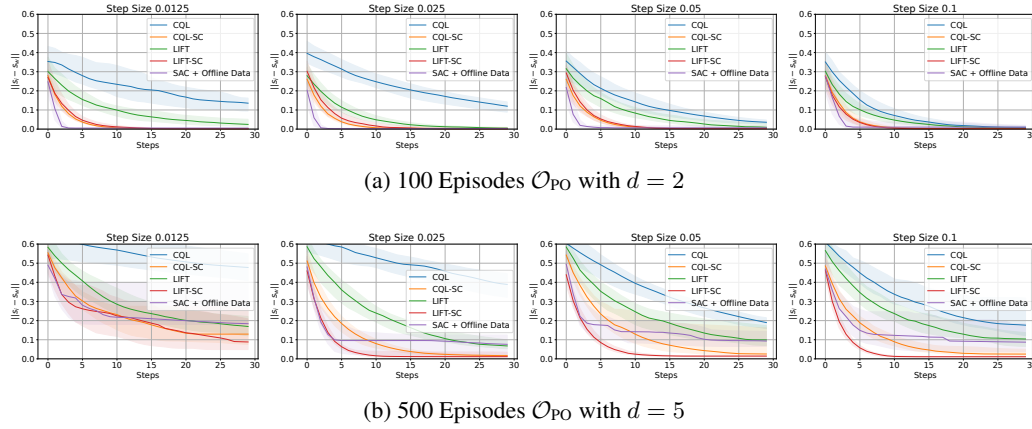
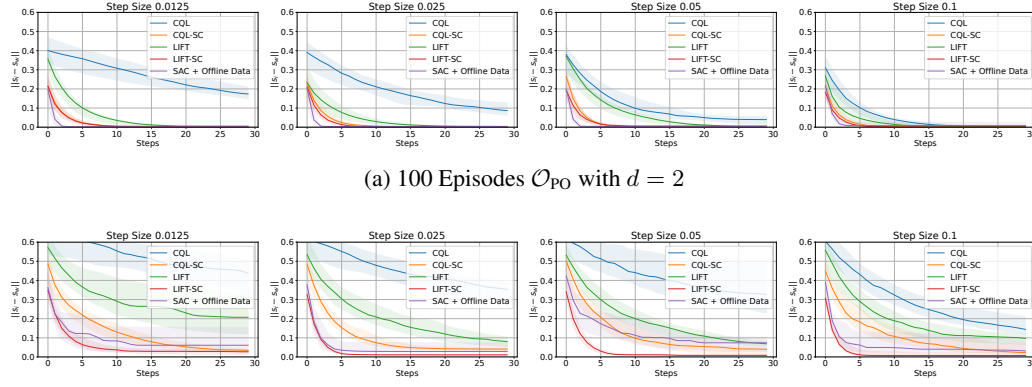
1183

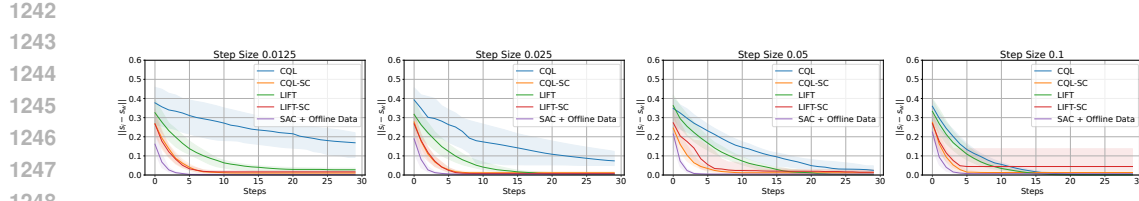
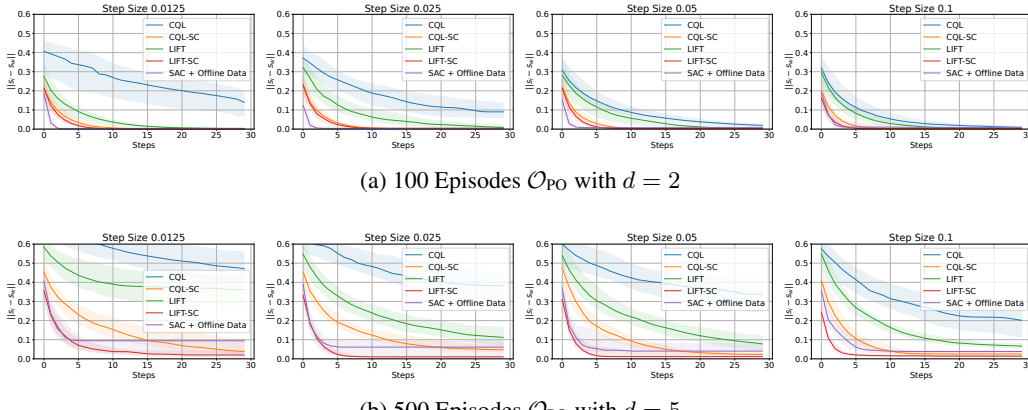
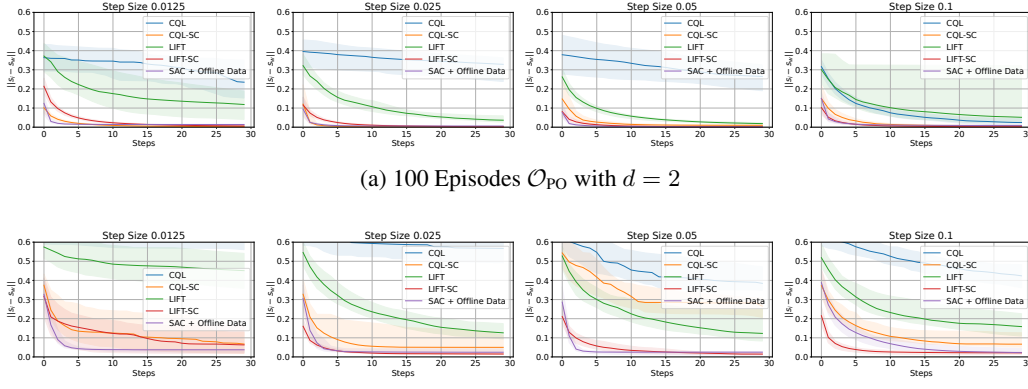
1184

1185

1186

1187

Figure 16: Experiments in  $f_{\text{blend}}$ .Figure 17: Experiments in  $f_{\text{scale}}$ .Figure 18: Experiments in  $f_{\text{rot}}$ .

Figure 19: Experiments in  $f_{\text{regrot}}$ .Figure 20: Experiments in  $f_{\text{sin}}$ .Figure 21: Experiments in  $f_{\text{sqrt}}$ .